REPORT NO. NADC-76387-30
CONTRACT N62269-75-C-0385

INVESTIGATION OF DAMAGE TOLERANCE OF GRAPHITE/EPOXY STRUCTURES AND RELATED DESIGN IMPLICATIONS

FINAL REPORT

REPORT DOCUMENTATION PAGE		READ INSTRUCTIONS BEFORE COMPLETING FORM
1. REPORT NUMBER NADC-76387-30	2. GOVT ACCESSION NO.	3. RECIPIENT'S CATALOG NUMBER
4. TITLE *(and Subtitle)* Investigation of Damage Tolerance of Graphite/Epoxy Structures and Related Design Implications		5. TYPE OF REPORT & PERIOD COVERED Final Report. July 1975 – November 1976
		6. PERFORMING ORG. REPORT NUMBER
7. AUTHOR(s) N. R. Adsit J. P. Waszczak		8. CONTRACT OR GRANT NUMBER(s) N62269-75-C-0385
9. PERFORMING ORGANIZATION NAME AND ADDRESS General Dynamics Convair Division P. O. Box 80847 San Diego, California 92138		10. PROGRAM ELEMENT, PROJECT, TASK AREA & WORK UNIT NUMBERS
11. CONTROLLING OFFICE NAME AND ADDRESS NADC Warminster, Pennsylvania		12. REPORT DATE 14 December 1976
		13. NUMBER OF PAGES 71
14. MONITORING AGENCY NAME & ADDRESS*(if different from Controlling Office)*		15. SECURITY CLASS. *(of this report)* Unclassified
		15a. DECLASSIFICATION/DOWNGRADING SCHEDULE N/A

16. DISTRIBUTION STATEMENT *(of this Report)*

Approved for public release; distribution unlimited.

17. DISTRIBUTION STATEMENT *(of the abstract entered in Block 20, if different from Report)*

18. SUPPLEMENTARY NOTES

19. KEY WORDS *(Continue on reverse side if necessary and identify by block number)*

graphite/epoxy construction, impact

20. ABSTRACT *(Continue on reverse side if necessary and identify by block number)*

This investigation was undertaken to evaluate the damage tolerance of typical
graphite/epoxy structure to service damage. AS/3501 graphite/epoxy I-stiffened
panels and honeycomb panels were fabricated and its tolerance to low-velocity
impacts was measured. → over

DD FORM 1473 EDITION OF 1 NOV 65 IS OBSOLETE
1 JAN 73

147650

20.

Three impact threats were investigated; runway stones, a blunt impactor with a tip radius of 0.64cm (1/4 inch), and a blunt impactor with a tip radius of 2.54cm (1 inch).

Impact parameters were selected that would just cause visual damage. This worked well for the runway stones, but for the tests of the one-inch penetrator on the honeycomb panels visual damage was not easily observed. C-scan damage was, however, easily detectable. Residual strength specimens were cut from the damaged panels and tested. The specimens contained damage at levels of 70, 100, 130% of the level to cause visual (or C-scan) damage.

The tensile residual strength of the I-stiffened panels (flat panels) decreased in relation to the energy of the impactor. The buckling and crippling strength of samples with a width-to-thickness ratio of 30 was not decreased. Tension-tension fatigue at 46 percent of ultimate did not fail the specimens. When these specimens were statically tested after 2.5×10^6 cycles, the residual strength was slightly increased from the corresponding tensile residual strengths.

For the damaged honeycomb specimens the more extensive the damage the lower the strength (tensile or compression) and the shorter the fatigue life. The tensile tests showed the same phenomena as the flat panels, i.e., the sharper the impactor the more severe the strength degradation for a given impact energy. However, in most cases degrading damage of the honeycomb is not even visible but needs to be detected by NDI techniques.

The design implications of these findings are only starting to be understood. Damage, even at the visual threshold level, can cause a substantial loss of load carrying ability of small residual strength specimens. More work needs to be performed to understand the exact mathematical relationship between the size of the damage and the degradation of the structure.

FOREWORD

This report was prepared by General Dynamics Convair Division, Advanced Composite Group, San Diego, California, under terms of Contract N62269-75-C-0385.

This final report covers the entire program from July 1975 through November 1976. The program was sponsored by the Air Vehicle Technology Department, Naval Air Development Center, Warminster, PA 18974. Mr. Lee W. Gause was the Project Engineer for NADC.

Dr. J. P. Waszczak was the original program manager, although Dr. N. R. Adsit completed the program as program manager and directed the testing.

The following Convair personnel also contributed to the program: M. Varlas and J. Hertz - panel fabrication, M. D. Campbell and G. L. O'Barr - impact tests and NDI, C. R. Maikish - machining, D. C. White - program control, E. Spier and H. McCutchen - stress analysis.

TABLE OF CONTENTS

LIST OF ILLUSTRATIONS

LIST OF ILLUSTRATIONS (continued)

LIST OF TABLES

SECTION 1

INTRODUCTION

Graphite/epoxy (G/E) is a composite structural material with outstanding stiffness and strength properties that make it useful for such applications as aircraft wing, tail, and fuselage skin panels. Design of the General Dynamics lightweight fighter aircraft (YF-16) specifies G/E panels in these areas, and General Dynamics Convair Division (GDC) has completed and reported on a fuselage composite conceptual design study[1] making use of this material for the Naval Air Development Center (NADC). However, a possible limitation to the application of G/E exists because of its lack of ductility, which may result in impact damage that is difficult to detect by visual inspection.

The research reported here was undertaken to evaluate the damage tolerance of G/E composite structures to manufacturing, handling, and service damage. An assessment of the damage tolerance of Type A-S/3501 G/E structural components to low-velocity impact threats was made, and the resulting design implications were identified.

To evaluate the low-velocity impact damage tolerance of G/E structures, two types of threats were selected for study: small tool drop impacts and runway stones. To simulate these real physical threats, a series of standardized tests was conducted. Two different spherical ended rods, having diameters 1.27 and 5.1 cm (0.5 inch and 2.0 inches), were selected to simulate the small tool drop threat. Standard size pea gravel was selected for use in the runway stone impact tests. All impact tests were run on large panels supported by reusable spar and rib substructure. The supported panels were representative of a typical Navy fighter wing design, thus eliminating the need to correct the test results for effects of finite size and edge support conditions, both of which relate directly to the dynamic response of the panel during impact. By systematically varying the mass, velocity, and shape of these impactors, a relationship was sought between damage type/magnitude and the impactor threat conditions (velocity, mass, shape).

The damaged structures were then carefully inspected both visually and using NDT methods to determine the type and extent of the physical damage. Specimens that included damaged structure were then machined from the damaged panels to run both residual strength and fatigue tests. Comparisons were made to similar data, run on undamaged control specimens taken from these same panels, to quantify material degradation due to the impact damage. The induced damage was modeled in such a way that analytical predictions could be made for residual strengths. These analytical

---

1.   F.F.W. Krohn et al, Model 200 Fuselage Composite Conceptual Design Study, NADC 75102-30, NADC, Warminster, PA, 12 December 1974.

predictions were compared to the experimental data to assess the theoretical model's applicability.

The experimental and analytical data was used as a basis to propose a number of different hardening techniques. The design implications arising from this investigation have been carefully reviewed and documented, and they are reported here. Suggested areas of required research identified during this study are also discussed.

SECTION 2

MATERIAL

2.1 SELECTION

The material chosen for this study was a low-modulus/ultra-high strength graphite-epoxy that is in use by the Navy on aircraft structures — type A-S/3501-5. The structural areas selected as representative for this study were the outer section of wings and lightly loaded sections of the empennage. In these areas the load is basically in one direction combined with shear and hence a layup of the family $[0/\pm45]_S$ was selected as representative.

To typify the construction that might be used for these areas it was decided to study both honeycomb panels (HCP) and I-stiffened panels (ISP). Therefore, both kinds of panels were made and are part of this study.

2.2 PANEL LAYUP AND QUALITY

Prepreg property tests were run on the type A-S/3501-5 material received from Hercules. The material, by supplier certification, met Hercules specifications HS-SG-500/2338 and HS-SG-500B. Convair's prepreg quality control test results, shown in Table 2-1, were in excellent agreement with the Hercules data.

All of the other material required for the program, i.e., 192 kg/m^3 (12.0 pcf) aluminum core, 88 kg/m^3 (5.5 pcf) HRP core, FM-123-5 film adhesive, and 3M EC-3500 B/A core splice adhesive, was ordered and received. Room temperature single lap shear tests were run on the FM-123-5 film adhesive. The results are reported in Table 2-2 and agree quite well with the vendor's reported average lap shear strength of 39.3 MPa (5700 psi).

Sixteen G/E laminates were laid up and cured with the following cure cycle.

1. Place vacuum bagged layup in autoclave.

2. Apply minimum vacuum of 84.65 kPa (25 inches of Hg).

3. At a rate of 1 to 3K/min, raise the laminate temperature 450 ±3K. During the heat-up, apply 585 +68, -0 kPa when the laminate temperature reaches 408 ±3K.

4. Hold at 84.65 kPa (25 inches Hg) (min), 585 +68, -0 kPa (85 +10, -0 psi), and 450 ±3K (350 ±5F) for 120 ±5 min.

5. Cool to below 339K (150F) at a rate not to exceed 3K/min.

2-1

Table 2-1. Receiving Inspection Quality Control Tests, Type A-S/3501-5
Graphite/Epoxy, Prepreg Properties

Property	Test Data	Average Value
Volatile Content	2.0% 1.3% 2.8%	2.0%
Resin Flow	20.8% 25.0% 21.8%	22.5%
Fiber Volume	60.83% 57.97% 55.87%	58.22%
Resin + Volatile Content	39.17% 42.03% 44.13%	41.78%
Average Resin Content	41.78% - 2.0%	39.78%

Table 2-2. Receiving Inspection Quality Control Tests, FM-123-5
Film Adhesive, Lap Shear Test

Specimen ID	Ultimate Lap Shear Strength (psi)	MPa
FM 1	5850	40.3
FM 2	6020	41.5
FM 3	6050	41.7
FM 4	5770	39.8
FM 5	6120	42.2
FM 6	5720	39.4
	$\overline{X}$ = 5922	40.8
	s = 164	1.13

6. Release autoclave vacuum and pressure.

7. Remove layup from autoclave.

8. Post cure laminate for two hours at 478K (400F) in air-circulating oven.

The relationship between laminate number and eventual panel use (ID) is shown in Table 2-3. Quality control tests run on each panel included two resin content, two specific gravity, three flexure, and three short beam shear tests. The results are summarized in Tables 2-4 and 2-5. The expressions used to calculate fiber volume and void content are also presented in Table 2-4. As is often the case, many of the calculated void contents are negative. This results from an accumulation of errors in the many physical measurements and calculations required to arrive at these figures. As discussed in Reference 2, while void contents less than 2% are considered acceptable for Type A-S/3501 G/E, it is desirable to achieve void contents below 1% to maximize 0-degree short beam shear strengths. All laminate void contents calculated and listed in Table 2-4 are below 1%. In fact, 13 of 16 are zero (i.e., negative). As a final check on laminate quality, metallurgical mounts were made from panels 3, 4, 8, 14, and 15 to enable visual inspection of these layups. Those laminates with calculated positive void contents (panels 8, 14, and 15) were used as bottom facesheets and were not impacted, even though the metallurgical mounts indicated void-free laminates. Figure 2-1 is a photograph of a typical panel.

A demonstration honeycomb panel measuring 35.6 by 36 cm (14.0 by 14.2 inches) was fabricated to test the honeycomb design and fabrication concept selected and to prove the structural acceptability of this design for the tests to be run by both NADC and Convair.

Having previously passed a visual examination and coin tap test, the demonstration honeycomb panel (HCP) was C-scanned ultrasonically. The results indicated a uniform bond line between the facesheet and the core. There was no apparent compatibility problem between the 3M 3500 core splice adhesive and the FM 123-5 film adhesive. A total of eight honeycomb panels using this proven concept, was made for Convair's impact studies.

---

2. M. J. Yokota, Low Cost Manufacturing Techniques for Composites, — In-Process Control, CASD-ERR-75-040, General Dynamics Convair Division, December 1975.

Table 2-3. Relationship Between Laminate Number and
Eventual Panel ID

Laminate Number	Number Plies	Panel ID
0	12*	ISP-5 & ISP-6
1	12	ISP-1 & ISP-2
2	12	ISP-3 & ISP-4
3	8**	Top Facesheet: HCP-1 & HCP-2
4	8	Bottom Facesheet: HCP-1 & HCP-2
5	8	Top Facesheet: HCP-3 & HCP-4
6	8	Bottom Facesheet: HCP-3 & HCP-4
7	8	Top Facesheet: HCP-5 & HCP-6
8 +	8	Bottom Facesheet: HCP-5 & HCP-6
9	8	Top Facesheet: HCP-7 & HCP-8
10	8	Bottom Facesheet: HCP-7 & HCP-8
11	8	Bottom Facesheet: NADC Specimens 1-26
12	8	Top Facesheet: NADC Specimens 1-26
13	8	Top Facesheet: NADC Specimens 27-50
14 +	8	Bottom Facesheet: NADC Specimens 27-50
15 +	8	Bottom Facesheet: NADC Specimens 1-26

* $(\pm 45/0_2/\overline{+45})_s$ laminate

** $(0/\pm 45/0)_s$ laminate

\+   Void contents > 0 ; Refer to Table 2-4.

Table 2-4. Laminate Fiber/Resin Content and Specific
Gravity Measurements

Panel	W_f	σ_c	V_f	Voids	V_r
0	-	-	-	-	-
1	69.82	1.590	62.30	-0.15	37.70
2	70.77	1.595	63.36	-0.12	36.64
3	70.70	1.598	63.28	-0.34	36.72
4	70.56	1.612	63.13	-1.29	36.87
5	71.35	1.600	64.01	-0.23	35.99
6	72.06	1.611	64.82	-0.66	35.18
7	69.58	1.603	62.03	-1.06	37.97
8 +	68.60	1.578	60.95	+0.17	38.88
9	67.53	1.592	59.77	-1.10	40.23
10	68.11	1.598	60.40	-1.27	39.60
11	69.40	1.599	61.83	-0.87	38.17
12	70.36	1.597	62.90	-0.40	37.10
13	71.11	1.597	63.74	-0.13	36.26
14 +	69.35	1.570	61.78	+0.94	37.28
15 +	70.09	1.582	62.60	+0.45	36.95
$\bar{X}$	69.96	1.595	62.46	-0.40	37.44
s	1.24	0.011	1.38	0.65	1.36

+ Void Contents > 0

W_f = percent fiber by weight

σ_c = specific gravity of composite

V_f = percent fiber by volume

Voids = percent voids by volume

V_r = percent resin by volume

σ_f = specific gravity of fiber = 1.76

σ_r = specific gravity of resin = 1.27

$$V_f = \frac{W_f}{W_f + \sigma_f \, W_r / \sigma_r}$$

$$\text{Voids} = 100 - \left[\frac{W_f \, \sigma_c}{\sigma_f} + \frac{W_r \, \sigma_c}{\sigma_r} \right]$$

Table 2-5. Receiving Inspection Quality Control Tests, Type A-S/3501
Graphite/Epoxy, Laminate Properties

Panel Number	Average Flex Strength (ksi)	MPa	Average Short Beam Shear Strength (ksi)	MPa
0	121	834	9.2	63.4
1	136	938	11.3	77.9
2	144	993	12.5	81.2
	$\bar{X} = 134.1$	924	$\bar{X} = 11.0$	75.8
	$s = 11.7$	80.6	$s = 1.7$	11.7
3	180	1241	12.2	84.1
4	196	1351	12.1	83.4
5	203	1400	11.1	76.5
6	175	1207	11.7	80.7
7	187	1289	11.3	77.9
8	176	1213	11.7	80.7
9	191	1317	12.0	82.7
10	190	1310	11.5	79.3
11	192	1324	12.2	84.1
12	182	1255	11.5	79.2
13	190	1310	10.7	73.8
14	191	1317	11.4	78.6
15	168	1158	11.2	77.2
	$\bar{X} = 186$	1282	$\bar{X} = 11.6$	80.0
	$s = 9.6$	66.2	$s = 0.5$	3.44
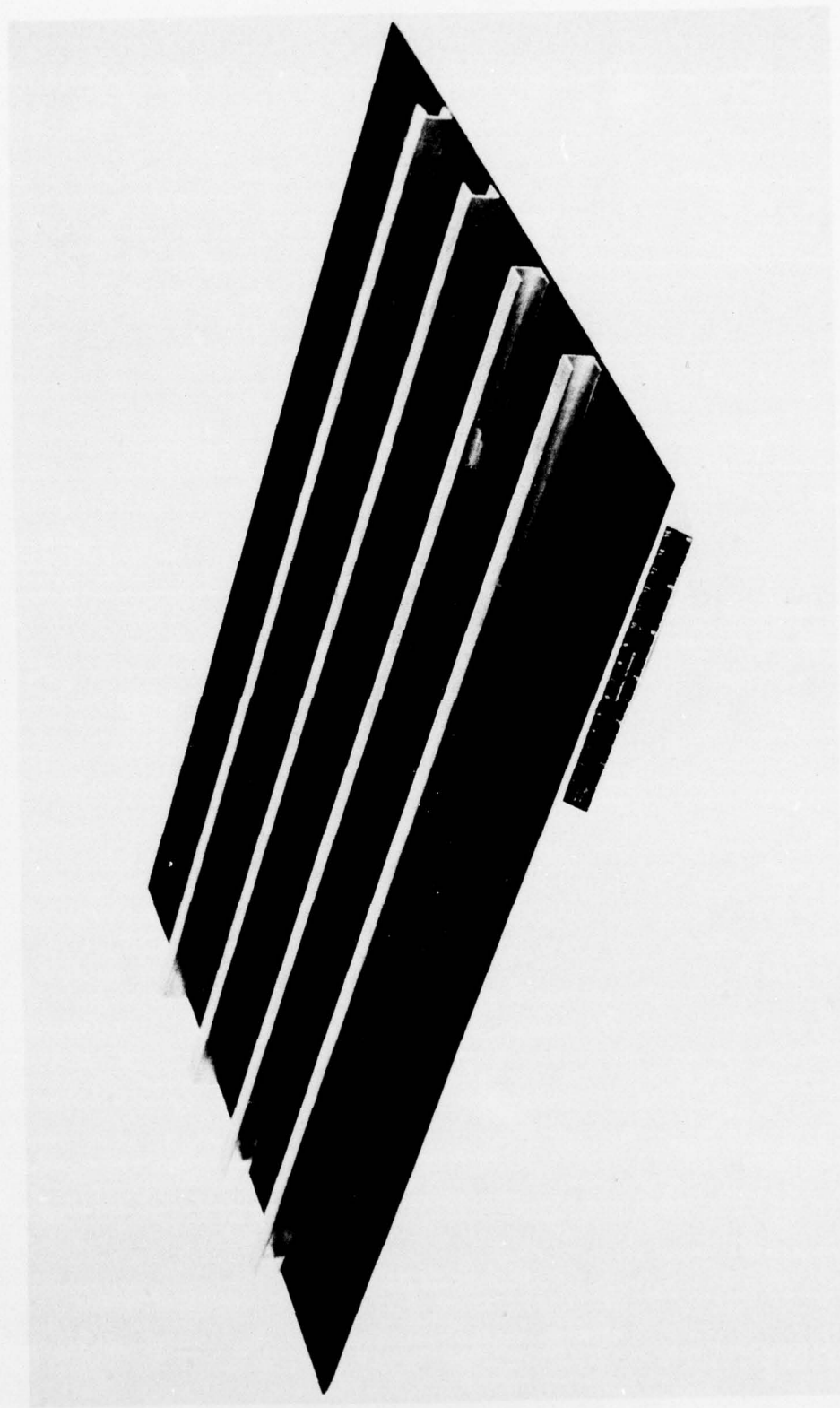
Figure 2-1. Typical Stiffened Graphite/Epoxy Panel

SECTION 3

TESTS, SPECIMENS, AND APPARATUS

A general summary of the test program is presented in Table 3-1. A total of 183 residual strength tests were run: 162 impact-residual strength tests and 21 undamaged control specimen tests. Of the 183 tests, 70 were strain gaged to monitor stiffness degradation.

The effects of the following variables on impact damage magnitude and material property degradation were studied: panel type (2), impact threat type (3), mass (3), and velocity (3). The two types of panel construction are I-stiffened (ISP) and honeycomb (HCP). Small tool drop threats and runway stones were identified as the impact threats of interest. To simulate the small tool drop threats, two different spherical ended rods with tip diameters of 1.22 cm (0.5 inch) and 5.04 cm (2.0 inch) were used. (See Figure 3-1). The impact velocities selected are representative of the threat conditions to which military aircraft are commonly exposed. The approximate required heights for the drop tests are also listed in Table 3-2. Selection of masses (m_1, m_2, m_3) was made by an initial series of screening tests. Assuming $m_1 < m_2 < m_3$, m_2 is the mass that represents visual threshold damage ($m_1 = 0.70\,m_2$ and $m_3 = 1.30\,m_2$).

The runway stone impact tests were run using small crushed granite stones, selected to satisfy both shape and weight specifications. The stones (Figure 3-1) were fired from a compressed air gun (Figure 3-2). Velocities were measured photo-electrically within the last foot of the stones flight path. Drop tests were performed using a 5 cm (2-inch) inside diameter tube to guide the penetrators to predetermined impact locations. The impact locations for the I-stiffened and honeycomb panels are shown in Figures 3-3 and 3-4 respectively. Along the edges of each panel a one-inch strip of material was utilized as support structure. The dotted lines indicate the boundaries of the various impact-residual strength test specimens.

All impact tests were performed on large panels supported by spar and rib substructure representative of typical Navy wing designs. In this manner the dynamic response of the G/E panels during impact simulated that which would be induced in an actual G/E wing. The spar and rib spacings selected are 41cm and 46cm (16 in. and 18 in.) respectively.

Specimen IDs for the 93 laminate tests (81 impact-residual strength tests and 12 controls) are listed in Table 3-3. The corresponding IDs for the 90 sandwich tests (81 impact-residual strength tests and 9 controls) are listed in Table 3-4. Details of the individual tension, compression, and fatigue specimens for the I-stiffened and sandwich panels are shown in Figures 3-5 and 3-6 respectively.

3-1

Table 3-1. Test Program Summary

Material   -   Type A-S/3501 Graphite/Epoxy
                 HRP Core, 88 kg/m^3 (5.5 pcf)
                 AF-143 Film Adhesive or FM-123
                 3M 3500 Core Potting

Layups   -   ISP $(\pm45/0_2/\mp45)_S$ 12 ply   1.5 mm (0.060 inch)
                 HCP $(0/\pm45/0)_S$ 8 ply   1.0 mm (0.040 inch)

Test Specimens:

		Tension	Compression	Fatigue	Total
Controls	ISP	4/4	4/4	4/0	12/8
	HCP	3/3	3/3	3/3	9/9
Damaged	ISP	27/15	27/10	27/0	81/25
	HCP	27/15	27/10	27/3	81/28
					183/70

Notation: Total Number/Number Gaged

Support Structure - 8 mm (5/16-inch) steel angle frame, 6.3 cm × 3.8 cm
                     (2 1/2 by 1 1/2 inches), 41 cm (16-inch) spar spacing,
                     46 cm (18-inch) rib spacing
                     Test panels attached to frame using C-clamps
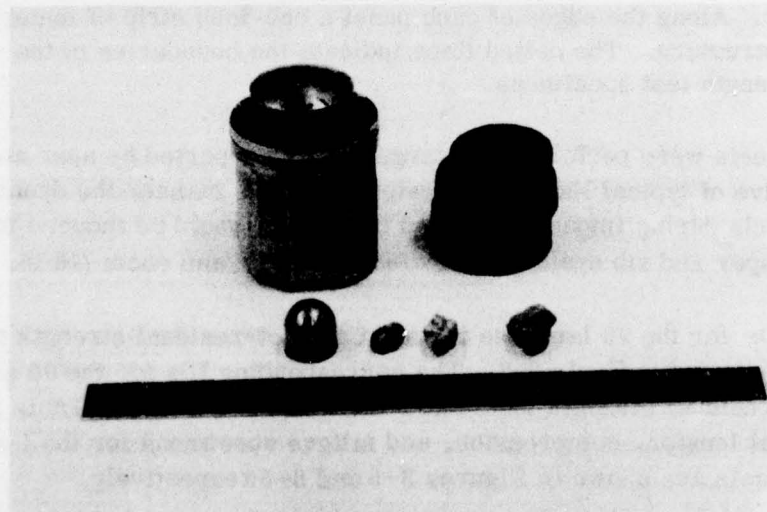
Figure 3-1. Impactors Used for Small Tool Threats and
             Runway Stones

3-2

Table 3-2. Impact Threat Parameters Used

Panel Type	Threat Type	Threat Parameters	
ISP	RS	m = 0.45 gm	v = 88.1, 103, 153 m/s
		m = 0.90 gm	v = 66.4, 88.4, 115 m/s
		m = 1.50 gm	v = 47.8, 64.0, 82.9 m/s
	R = 0.63 cm (1/4 in.)	h = 1.22 m (4 ft)	m = 108, 140.4, 182.5 gm
		h = 2.74 m(9 ft)	m = 71, 92.3, 120 gm
		h = 6.1 m (20 ft)	m = 38, 49.4, 64.2 gm
	R = 2.54 cm (1 in.)	h = 1.22 m (4 ft)	m = 159, 206.7, 268.7 gm
		h = 2.74 m (9 ft)	m = 100, 130, 169 gm
		h = 6.1 m (20 ft)	m = 70, 91, 118.3 gm
HCP	RS	m = 0.45 gm	v = 53.6, 71.6, 93.3 m/s
		m = 0.90 gm	v = 40.5, 53.9, 70.1 m/s
		m = 1.50 gm	v = 29.3, 39.0, 50.6 m/s
	R = 0.63 cm (1/4 in.)	h = 1.22 m (4 ft)	m = 81, 108, 140.4 gm
		h = 2.74 m (9 ft)	m = 53.3, 71, 92.3 gm
		h = 6.1 m (20 ft)	m = 28.5, 38.0, 49.4 gm
	R = 2.54 cm (1 in.)	h = 1.22 m (4 ft)	m = 119.3, 159, 206.7 gm
		h = 2.74 m (9 ft)	m = 75, 100, 130 gm
		h = 6.1 m (20 ft)	m = 52.5, 70, 91 gm

RS
R = 0.63 cm (1/4 in.)
R = 2.54 cm (1 in.)

Runway Stones
Blunt Penetrator (small), 0.63 cm (1/4 in.) Tip Radius
Blunt Penetrator (large), 2.54 cm (1 in.) Tip Radius

3-3
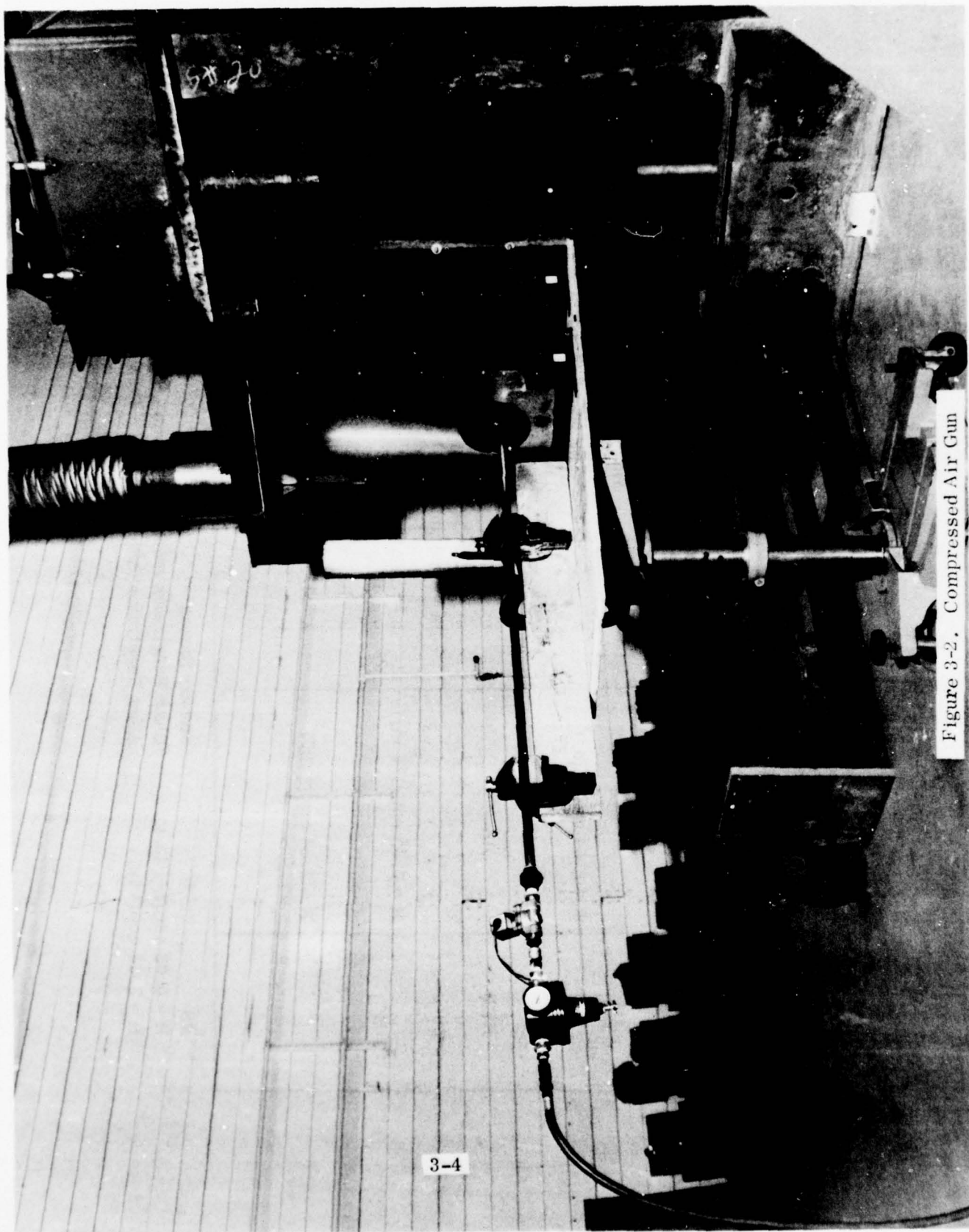
Figure 3-2. Compressed Air Gun

3-4
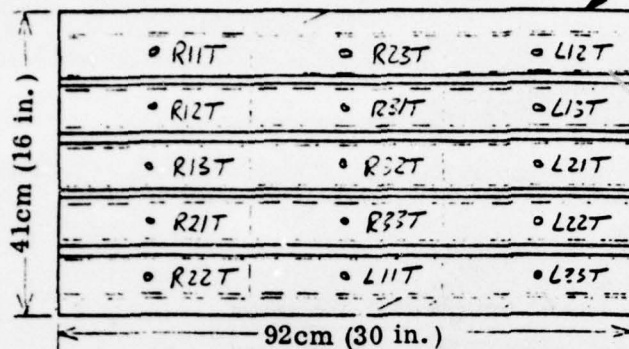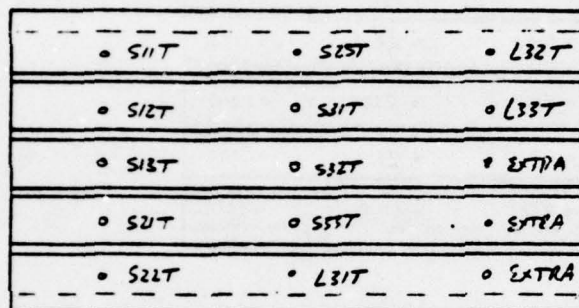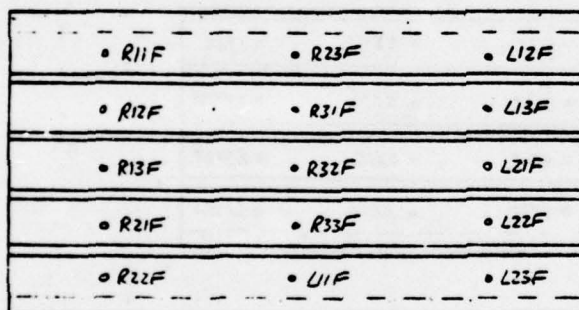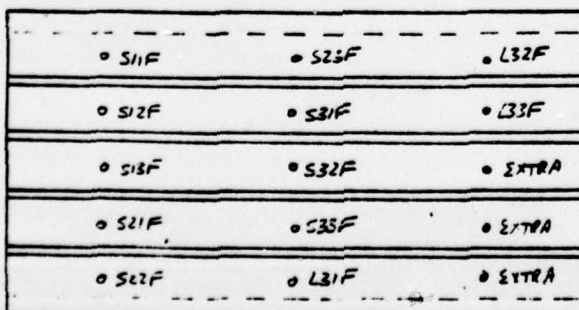
ISP-1

Area supported during impact tests

○ R11T	○ R23T	○ L12T
○ R12T	○ R31T	○ L13T
○ R13T	○ R32T	○ L21T
○ R21T	○ R33T	○ L22T
○ R22T	○ L11T	○ L23T

← 41cm (16 in.) →
← 92cm (30 in.) →

ISP-2

○ S11T	○ S25T	○ L32T
○ S12T	○ S31T	○ L33T
○ S13T	○ S32T	○ EXTRA
○ S21T	○ S55T	○ EXTRA
○ S22T	○ L31T	○ EXTRA

ISP-3

Detailed specimen layout pattern only shown for ISP-1 and ISP-5

○ R11F	○ R23F	○ L12F
○ R12F	○ R31F	○ L13F
○ R13F	○ R32F	○ L21F
○ R21F	○ R33F	○ L22F
○ R22F	○ L11F	○ L23F

$(\pm 45/0_2/\mp 45)_s$, 1.5 mm (0.060 in.)

33% 0's

ISP-4

○ S11F	○ S23F	○ L32F
○ S12F	○ S31F	○ L33F
○ S13F	○ S32F	○ EXTRA
○ S21F	○ S35F	○ EXTRA
○ S22F	○ L31F	○ EXTRA

↔ 5.0 cm (2 in.)

Figure 3-3. I-Stiffened Impact Panels – Specimen Layout

3-5

ISP-5

61 cm (24 in.)

41 cm (16 in.)

• R11C	• R23C	• L12C
• R12C	• R31C	• L13C
• R13C	• R32C	• L21C
• R21C	• R33C	• L22C
• R22C	• L11C	• L23C

ISP-6

• S11C	• S23C	• L32C
• S12C	• S31C	• L33C
• S13C	• S32C	• EXTRA
• S21C	• S33C	• EXTRA
• S22C	• L31C	• EXTRA
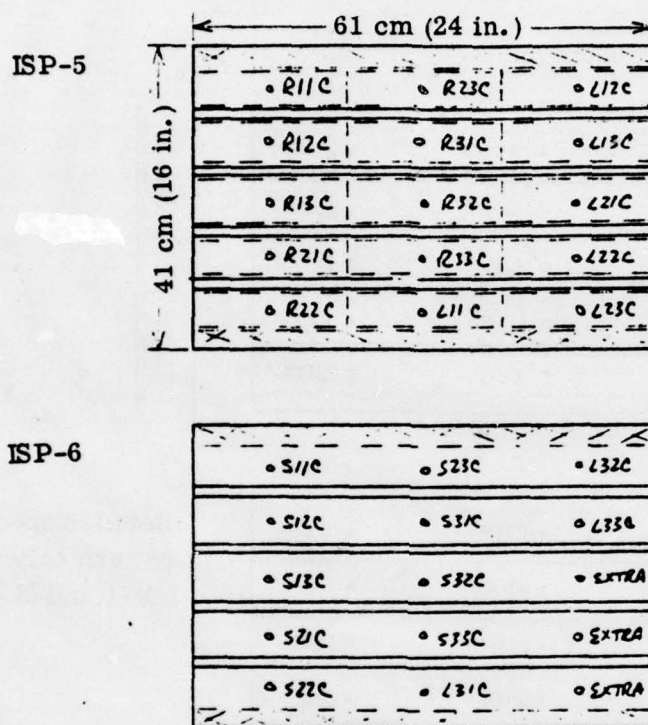
Figure 3-3.   I-Stiffened Impact Panels – Specimen Layout (Cont'd)
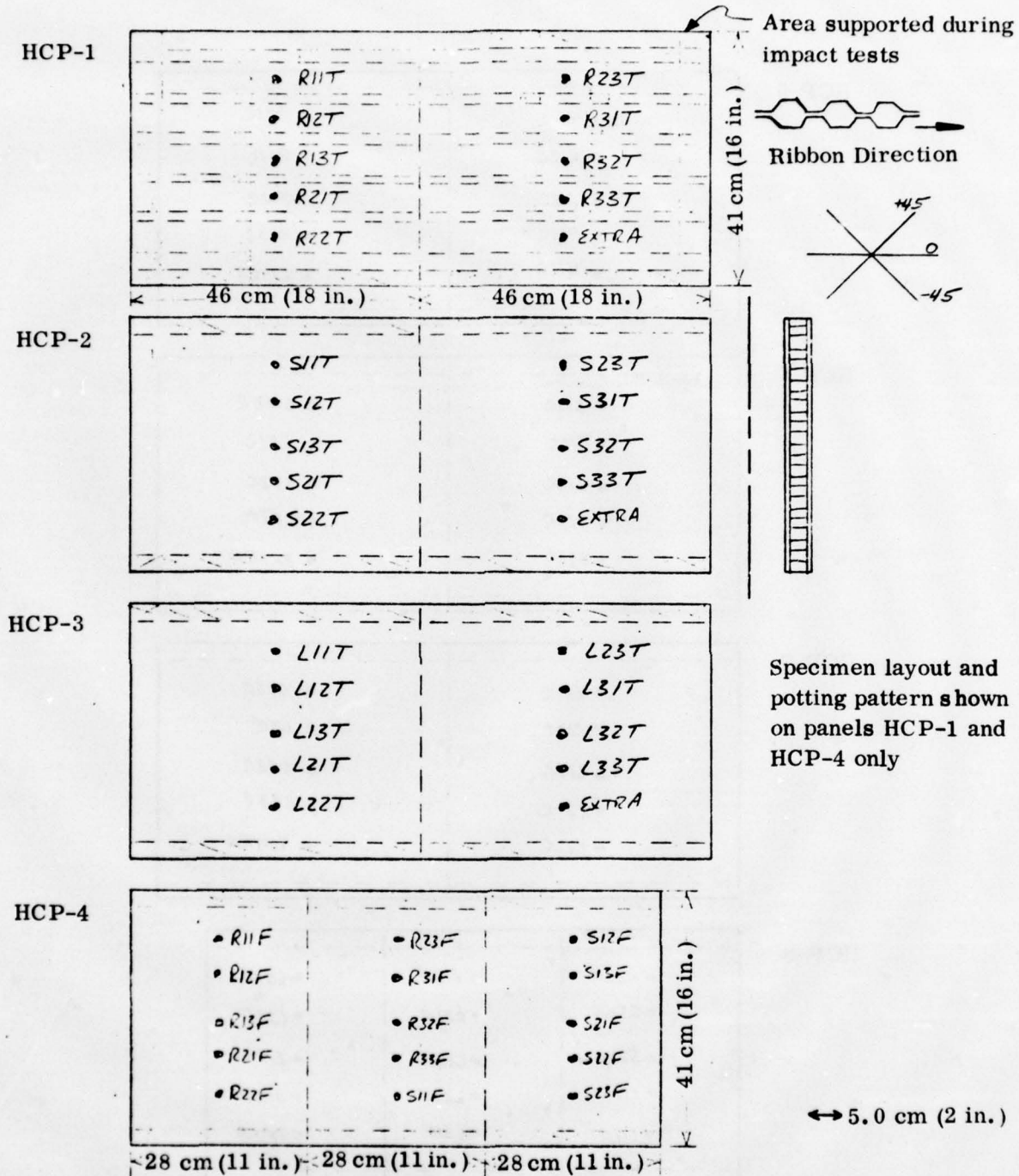
Figure 3-4. Honeycomb Impact Panels – Specimen Layout

HCP-5

R11C	R23C
R12C	R31C
R13C	R32C
R21C	R33C
R22C	EXTRA

HCP-6

S11C	S23C
S12C	S31C
S13C	S32C
S21C	S33C
S22C	EXTRA

HCP-7

L11C	L23C
L12C	L31C
L13C	L32C
L21C	L33C
L22C	EXTRA

HCP-8

S31F	L13F	L32F
S32F	L21F	L33F
S33F	L22F	EXTRA
L11F	L23F	EXTRA
L12F	L31F	EXTRA

Figure 3-4. Honeycomb Impact Panels – Specimen Layout (Cont'd)

3-8

Table 3-3. Scheduled Laminate Tests (ISP)

Impact-Residual Strength Tests			Controls
IR11T	IS11T	IL11T	c I1T
IR11C	IS11C	IL11C	c I1C
IR11F	IS11F	IL11F	c I1F
IR12T	IS12T	IL12T	c I2T
IR12C	IS12C	IL12C	c I2C
IR12F	IS12F	IL12F	c I2F
IR13T	IS13T	IL13T	c I3T
IR13C	IS13C	IL13C	c I3C
IR13F	IS13F	IL13F	c I3F
IR21T	IS21T	IL21T	c I4T
IR21C	IS21C	IL21C	c I4C
IR21F	IS21F	IL21F	c I4F
IR22T	IS22T	IL22T	
IR22C	IS22C	IL22C	
IR22F	IS22F	IL22F	
IR23T	IS23T	IL23T	
IR23C	IS23C	IL23C	
IR23F	IS23F	IL23F	
IR31T	IS31T	IL31T	
IR31C	IS31C	IL31C	
IR31F	IS31F	IL31F	
IR32T	IS32T	IL32T	
IR32C	IS32C	IL32C	
IR32F	IS32F	IL32F	
IR33T	IS33T	IL33T	
IR33C	IS33C	IL33C	
IR33F	IS33F	IL33F	

R = Runway Stone   T = Tension

S = Small Blunt (D = 1.27cm (0.5 in.)   C = Compression

L = Large Blunt (D = 5.0cm (2.0 in.)   F = Fatigue

I = I-Stiffened Panel   c = Control

Example Notation:

Panel Type-Threat-Mass-Velocity-Test

IR23C = I-Stiffened Panel, Runway Stone Impact, Mass No. 2,
Velocity No. 3, Compression

Table 3-4. Scheduled Sandwich Tests (HCP)

Impact-Residual Strength Tests			Controls
HR11T	HS11T	HL11T	c H1T
HR11C	HS11C	HL11C	c H1C
HR11F	HS11F	HL11F	c H1F
HR12T	HS12T	HL12T	c H2T
HR12C	HS12C	HL12C	c H2C
HR12F	HS12F	HL12F	c H2F
HR13T	HS13T	HL13T	c H3T
HR13C	HS13C	HL13C	c H3C
HR13F	HS13F	HL13F	c H3F
HR21T	HS21T	HL21T	
HR21C	HS21C	HL21C	
HR21F	HS21F	HL21F	
HR22T	HS22T	HL22T	
HR22C	HS22C	HL22C	
HR22F	HS22F	HL22F	
HR23T	HS23T	HL23T	
HR23C	HS23C	HL23C	
HR23F	HS23F	HL23F	
HR31T	HS31T	HL31T	
HR31C	HS31C	HL31C	
HR31F	HS31F	HL31F	
HR32T	HS32T	HL32T	
HR32C	HS32C	HL32C	
HR32F	HS32F	HL32F	
HR33T	HS33T	HL33T	
HR33C	HS33C	HL33C	
HR33F	HS33F	HL33F	

R = Runway Stone   T = Tension
S = Small Blunt (D = 1.27cm (0.5 in.)   C = Compression
L = Large Blunt (D = 5.0cm (2.0 in.)   F = Fatigue
H = Honeycomb Panel   c = Control

Example Notation:
Panel Type - Threat-Mass-Velocity-Test
HL31F = Honeycomb Panel, Large Blunt
Penetrator, Mass No. 3, Velocity No. 1, Fatigue
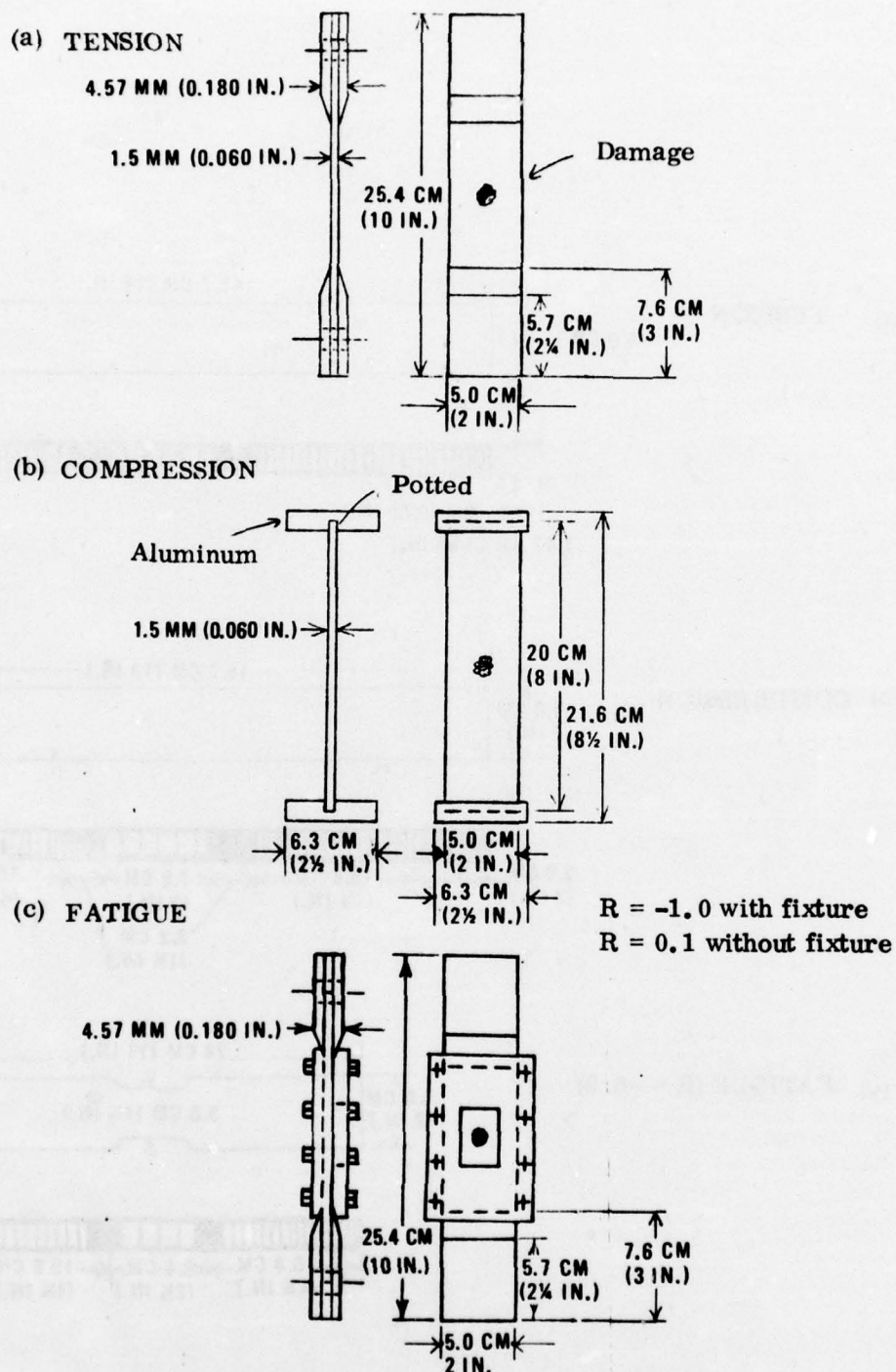
Figure 3-5. Laminate (ISP) Test Specimen Configurations

(a) TENSION

45.7 CM (18 IN.)

5.0 CM (2 IN.)

1.27 CM (0.50 IN.)
1.47 CM (0.58 IN.)

(b) COMPRESSION

45.7 CM (18 IN.)

5.0 CM
2 IN.)

5.0 CM
(2 IN.)   10.8 CM
(4¼ IN.)   7.6 CM
(3 IN.)   10.8 CM
(4¼ IN.)

3.2 CM
(1¼ IN.)

5.0 CM
(2 IN.)

(c) FATIGUE (R = -0.9)

28 CM (11 IN.)

5.0 CM
(2 IN.)   3.8 CM (1½ IN.)

10.8 CM
(4¼ IN.)   6.4 CM
(2½ IN.)   10.8 CM
(4¼ IN.)
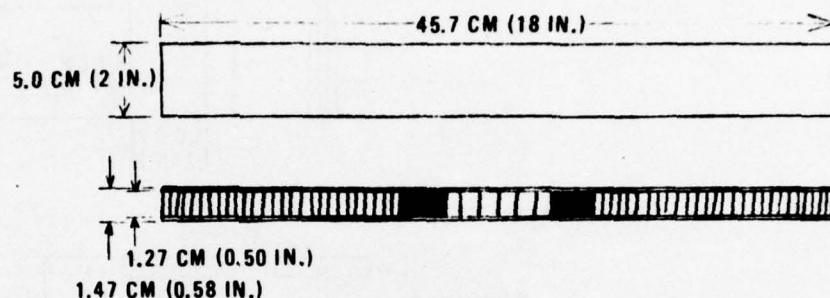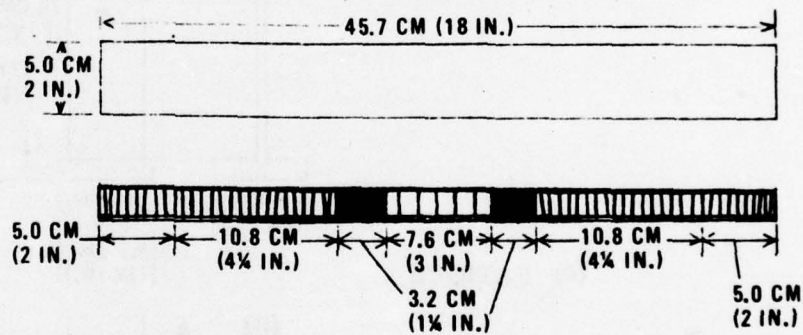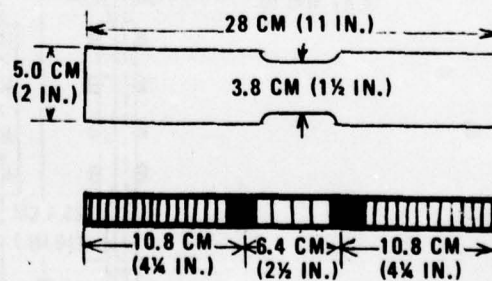
Figure 3-6. Honeycomb (HCP) Test Specimen Configurations

The tensile tests of laminates (Figure 3-5a) were run in a Universal test machine with wedge action jaws to grip the specimen. The residual strength tests from the fatigue tests were run in the same machine. The compression test was actually a crippling test that has been used at Convair extensively. The test setup is shown in Figure 3-7. This specimen has a breadth-to-thickness ratio (b/t) of 30. With such a ratio one measures the crippling strength rather than compression (b/t < 10) or buckling (1/ρ > 50) (where ρ is radius of gyration). The fatigue tests were all run on Sontag SF-1U high-cycle fatigue test machines. Some original tests were run with both tension and compression loads using the fixture sketched in Figure 3-5c, but because of fixture problems the remainder of the tests were run with only tension-tension fatigue and the fixture was not used.

The static tests of the HCP specimens were run all using the same basic specimen (Figure 3-6). Those were all four-point loading bending beams with the skins in tension (bottom) and compression (top) (Figure 3-8). This worked adequately for the tension tests because the specimens failed in tension. In compression an extra aluminum metal sheet 2.0 mm (0.080 inch) was bonded to the bottom sheet to force the failure into the compression skin (top).

The fixture tests of HCP fatigue specimens were the most difficult, and the final method was to test the specimen in a closed-loop test machine at a slow frequency (< 1 Hz). The test setup is shown in Figure 3-9. It was also found that the specimen had to be necked slightly in the test section as shown in Figure 3-6c to force the failure into that section rather than in the bond line in the core.

The modulus of elasticity (stiffness) of selected specimens was determined from data obtained by using strain gages. Gages were all Baldwin Lima Hamilton gages of the FAE type bonded to the samples with contact adhesive (Eastman 910).
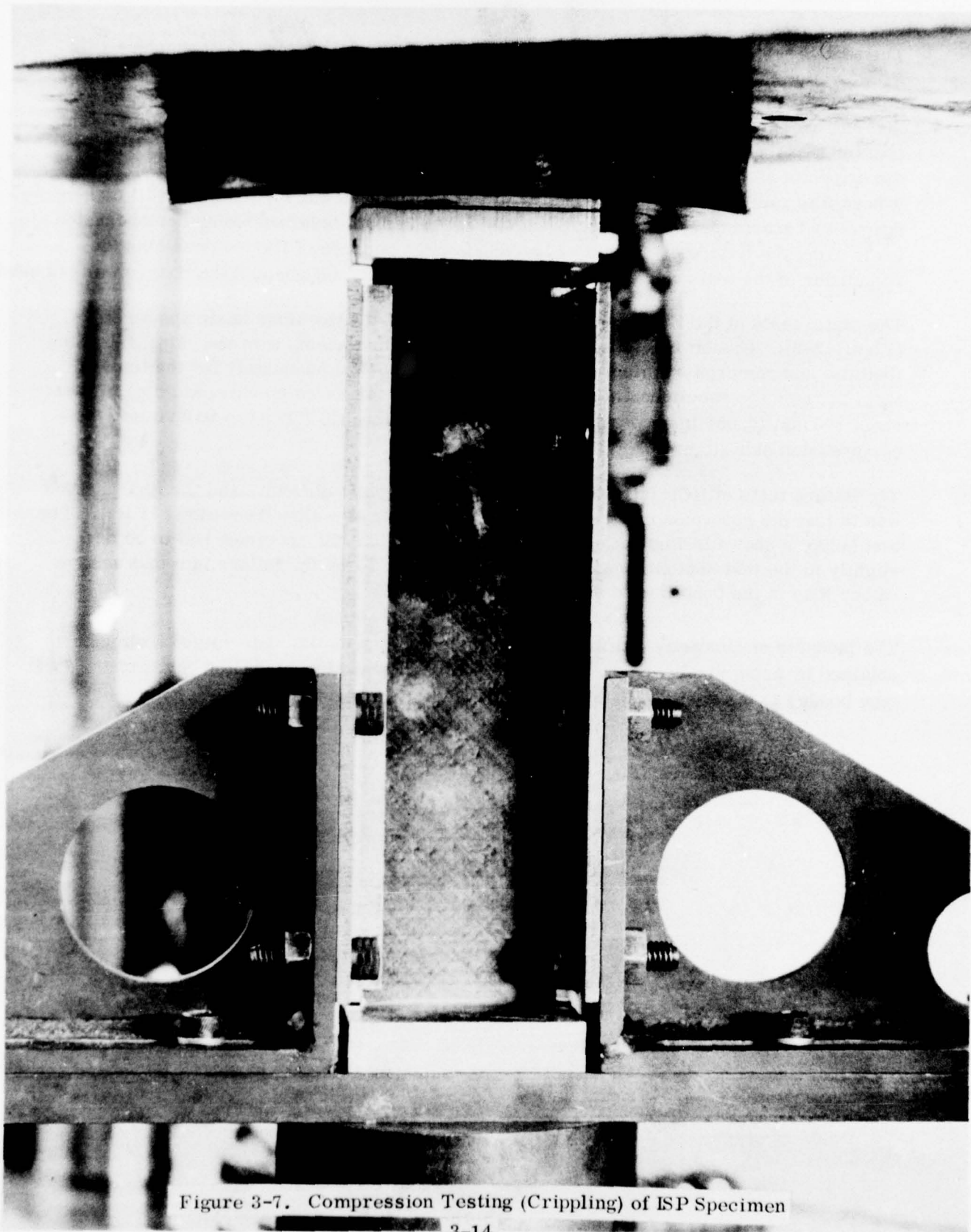
Figure 3-7. Compression Testing (Crippling) of ISP Specimen
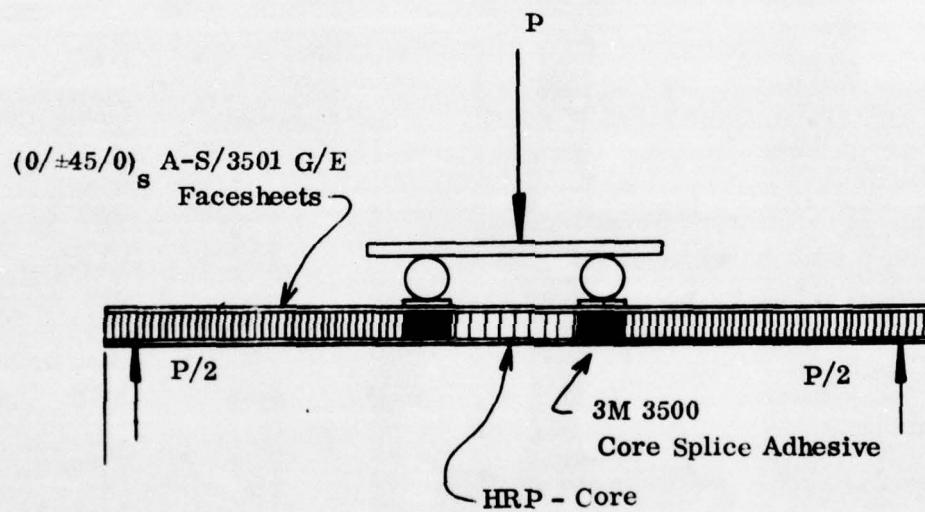
Figure 3-8. Four Point Bend Test Specimen Loading Method
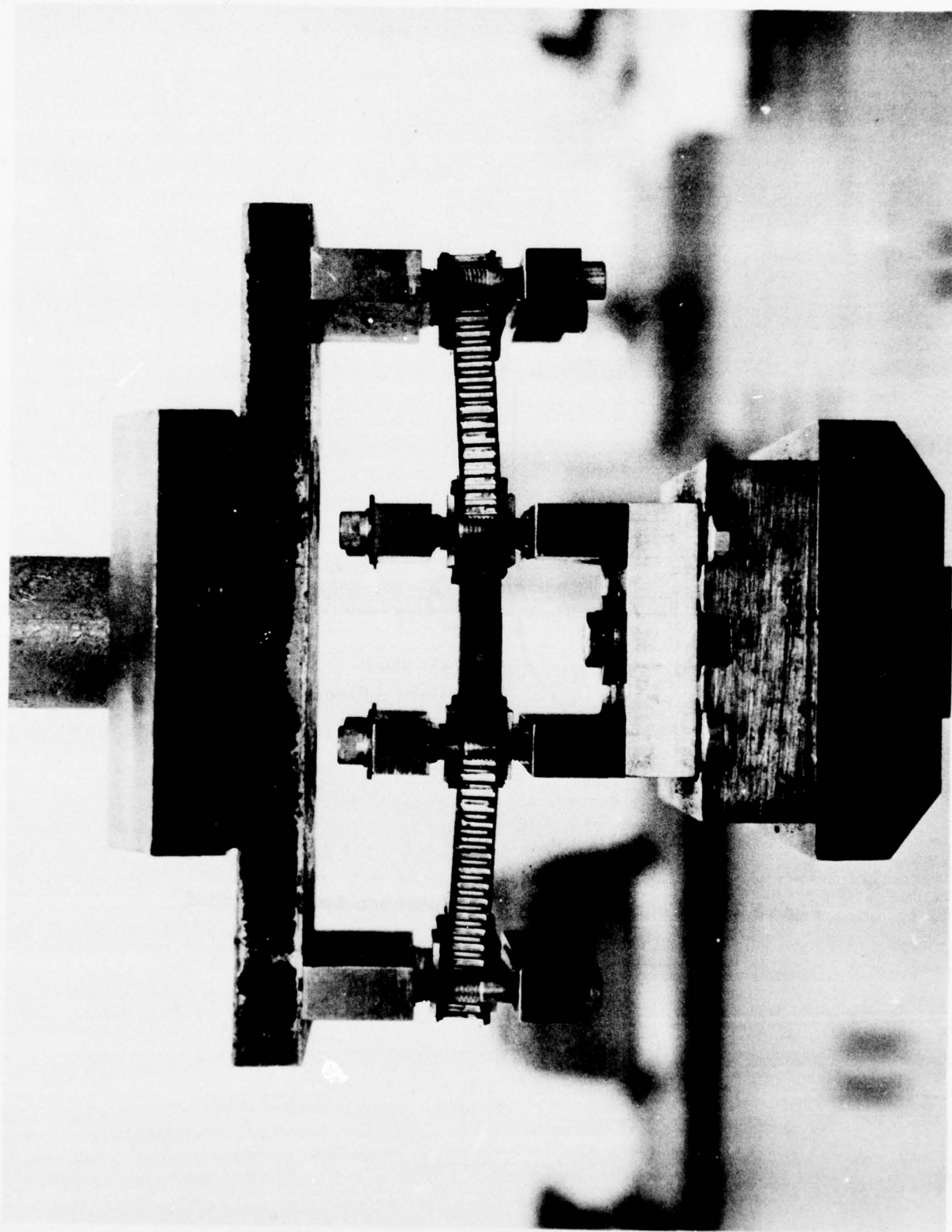
Figure 3-9. Fatigue Test Setup for HCP Specimens

SECTION 4

RESULTS

4.1   DAMAGE

Following completion of the impact test phase, each damage site was closely inspected
and the damage magnitude, both visual and C-scan, was measured and recorded. The
damage magnitude for the 81 impacts on the stiffened laminate panels is summarized
in Table 4-1. Similar data for the 81 honeycomb panel impact tests is summarized
in Table 4-2. It is clear that the magnitude of damage which is visually detectable is
much less than that which can be observed using ultrasonic C-scan methods. In many
cases, especially for the large blunt impactors, while visual damage was not easily
observed, significant damage could be detected using C-scan. In a number of cases
the detection of visual damage, which was less than 5 mm by 5 mm (C-scan) in size,
was often very difficult and questionable.

Figures 4-1, 4-2, and 4-3 illustrate the types and magnitudes of visual damage
observed. In Figure 4-1, a series of three specimens is presented in which the
damage magnitude varies from below threshold (specimen ISP-2) to above threshold
(specimen ISP-8). These three examples represent runway stone impact damage.
As can be seen from the photographs, the front face damage for each impact could be
observed and took the form of minor scuffs, scratches, and dents. In Figure 4-2, typical
above threshold damage for the R = 0.63 cm (1/4-inch) and R = 2.54 cm (1-inch) blunt pene-
trators is illustrated. Only back face damage has been shown since no front face damage
exists in either case. To be consistent with the runway stone damage, all visual observa-
tions and measurements for the solid laminate specimens were made using back face
damage only. Typical above threshold damage for the graphite/epoxy honeycomb panels is
illustrated in Figure 4-3a and b for both runway stone impacts and the R = 0.63 cm (1/4-
inch) blunt penetrator. While both of these examples show relatively small impact damage
impressions, this damage does represent the most readily observed for the honeycomb
panels. Threshold and below threshold damage for the sandwich structures could not
be visually observed, even though ultrasonic C-scan inspection of the panels indicated
large damage sites as listed in Table 4-2. More severe impact threats were not
imposed on these panels to induce visual damage since the C-scan damage was already
significant and it was expected that large degradations in at least compression strength
would result.

4.2   TEST (RESIDUAL STRENGTH, STIFFNESS, FATIGUE)

A summary of the residual tension and compression strengths for the honeycomb test
specimens is presented in Tables 4-3 and 4-4 respectively. Photographs of typical
failed specimens in tension and compression are presented in Figure 4-4 and 4-5
respectively.

4-1

Table 4-1. Damage Magnitude for Impacts on Stiffened Laminate Panels

Runway Stones			R=0.63cm (1/4 in.) Impactor			R=2.54cm (1-in.) Impactor		
Spec. No.	Visual[1] (mm)	C-Scan (mm)	Spec. No.	Visual[1] (mm)	C-Scan (mm)	Spec. No.	Visual[1] (mm)	C-Scan (mm)
1	1×3	14×14	28a	–	– ?	55a	–	4×12
2*	–	9×9	29a	–	7×11	56a	–	–
3	–	11×11	30a	–	–	57a	3×3	–
4a	– ?	7×7	31	–	1×1 ?	58	–	–
5a*	2×15	15×25	32	–	–	59	–	5×5 ?
6a	– ?	10×13	33	–	–	60	–	–
7	14×50	20×55	34	–	5×5 ?	61	–	–
8*	8×30	20×48	35	–	4×4 ?	62	–	6×6
9	5×57	73×53	36	–	5×5	63	–	5×5 ?
10	–	13×13	37a	3×8	8×15	64a	3×7	5×15
11	–	10×10	38a	–	5×6	65a	–	9×9
12	–	9×9	39a	2×7	9×16	66a	2×2	5×12
13	4×17	13×13	40	–	3×3 ?	67	–	–
14	5×45	12×48	41	–	–	68	–	9×9
15	2×12	14×14	42	–	–	69	–	8×8
16	9×46	16×40	43	–	5×5 ?	70	–	3×11
17	5×63	18×58	44	–	–	71	–	8×8
18	9×80	13×83	45	3×3	9×9	72	–	5×15
19	–	3×3	46a	–	– ?	73a	2×7	7×16
20	–	3×3	47 a*	2×14	10×12	74a*	3×23	11×27
21	–	5×5	48a	2×14	6×12	75a	–	7×20
22	–	8×8	49	–	– ?	76	–	11×11
23	4×24	10×24	50	–	3×3 ?	77	–	7×7
24	3×27	9×21	51	–	7×7	78	1×1	5×21
25	4×25	11×21	52	–	5×5 ?	79	1×1	11×11
26	–	15×15	53	–	5×5	80	–	8×8
27	5×43	14×45	54	–	5×5	81	2×6	6×22

1 Damage observed on back face of impacted laminate. All runway stone impacts left minor scuff marks on the impact surface.

? Indicates a questionable observation.

* Photograph of damage included in this report.

a Denotes two impacts for this specimen; the first impact did not induce damage (visual on C-scan).

25.4 mm = 1 inch

Table 4-2. Damage Magnitude for Impacts on Honeycomb Panels

Runway Stones			R=0.63cm (1/4 in.) Impactor			R=2.54cm (1-in.) Impactor		
Spec. No.	Visual[1] (mm)	C-Scan (mm)	Spec. No.	Visual[1] (mm)	C-Scan (mm)	Spec. No.	Visual[1] (mm)	C-Scan (mm)
1	1×3	3×10	28	–	3×11	55	– ?	5×12
2	– ?	4×9	29	1×1 ?	8×14	56	–	8×14
3	2×3	4×8	30	–	6×12	57	–	12×15
4	2×2	6×10	31	2×2 ?	4×14	58	– ?	12×22
5	4×4	6×12	32	3×3	5×12	59	–	10×10
6	1×2	7×8	33	3×3 ?	6×14	60	–	15×25
7	4×6	7×11	34	2×2 ?	6×18	61	– ?	14×23
8	2×4	8×12	35	6×6	5×13	62	–	13×14
9	3×4	6×10	36	4×4	8×15	63	–	14×19
10	3×4	5×10	37	2×2 ?	6×13	64	– ?	9×13
11	2×2 ?	7×13	38	2×2 ?	5×13	65	–	10×14
12	3×3	4×7	39	3×3	5×12	66	–	10×15
13	2×4	5×11	40	5×5	8×16	67	– ?	16×22
14	3×3	6×10	41	5×5	7×12	68	– ?	15×25
15	2×2	6×11	42	5×5	5×13	69	–	14×29
16	3×4	8×12	43	7×7	11×16	70	– ?	10×26
17	3×5	7×11	44	5×9	9×20	71	– ?	16×24
18	2×2	7×14	45	6×6	10×25	72	–	14×29
19	1×3	3×10	46	2×2 ?	4×14	73	– ?	13×21
20	– ?	5×10	47	4×5 ?	4×12	74	– ?	15×28
21	–	5×9	48	3×3 ?	10×18	75	–	15×17
22	2×3	5×10	49	4×4	5×15	76	– ?	15×26
23	2×3	5×11	50	4×4 ?	4×13	77	– ?	12×19
24	3×3	7×14	51	5×5	14×20	78	–	14×25
25	3×3	6×12	52	7×7	8×18	79	– ?	17×30
26	3×5	8×12	53	8×8	8×13	80	– ?	18×31
27*	4×6	5×13	54*	7×7	10×20	81	–	16×28

1 Damage observed on the surface of the face sheet which was impacted.

? Indicates that observation of visual damage is questionable.

* Photograph of damage included in this report. Refer to previous bi-monthly for photograph of C-Scan damage.

25.4 mm = 1 inch
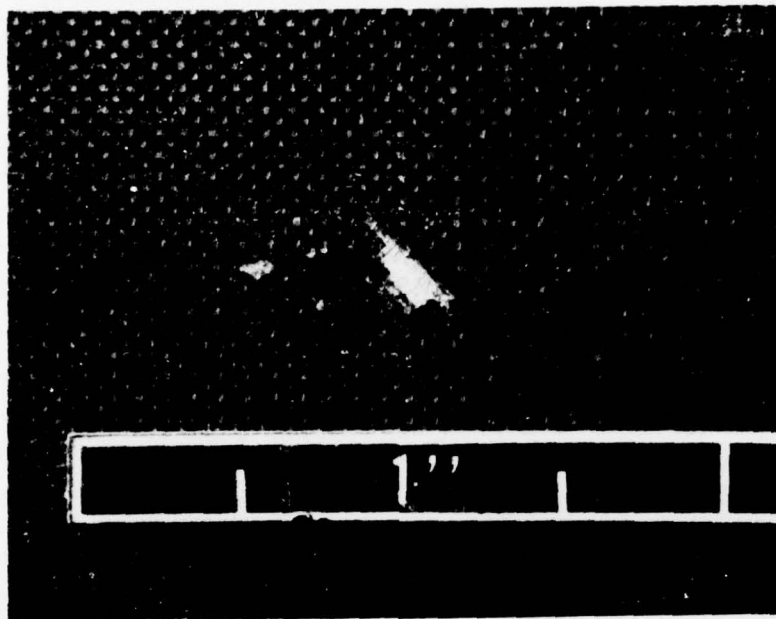
Front Face
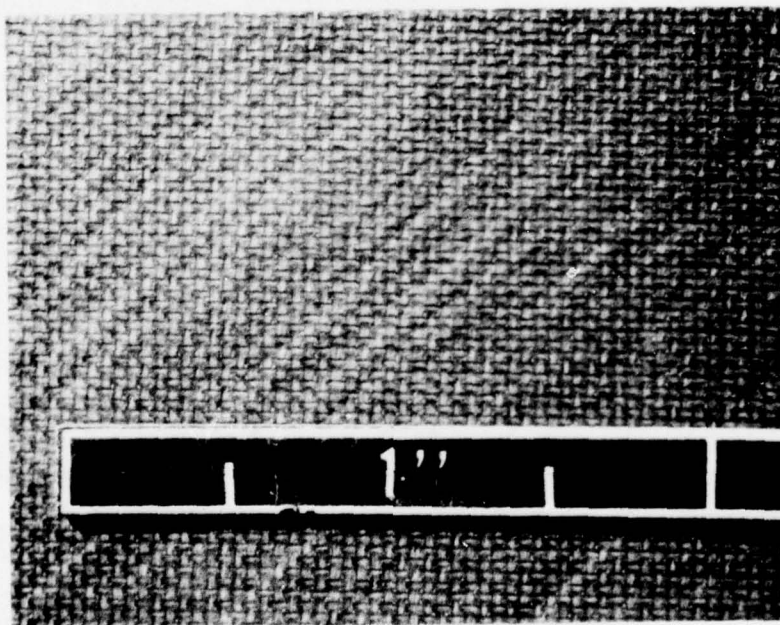
Back Face

Specimen ISP-2

Figure 4-1a. Typical Runway Stone Damage for 12 Ply G/E; Below Threshold

4-4
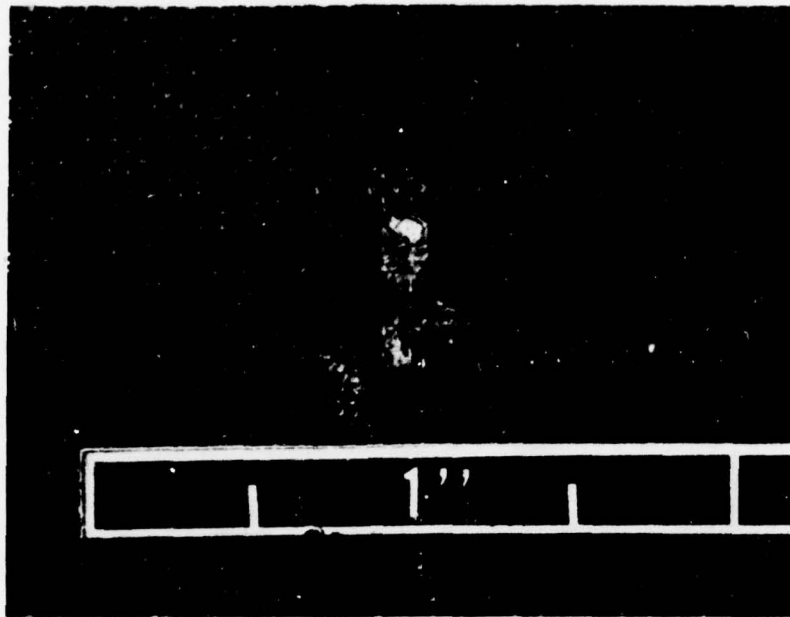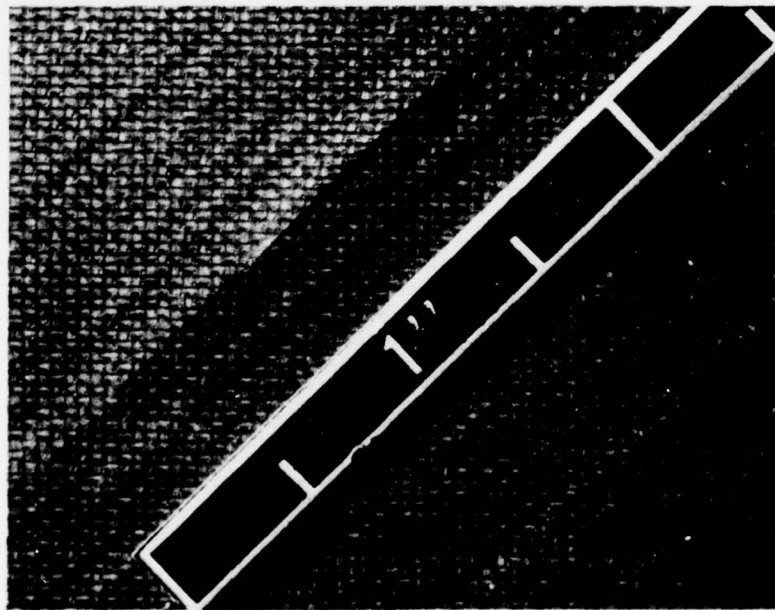
Front Face

Back Face

Specimen ISP-5a

Figure 4-1b.   Typical Runway Stone Damage for 12 Ply G/E; Threshold

4-5
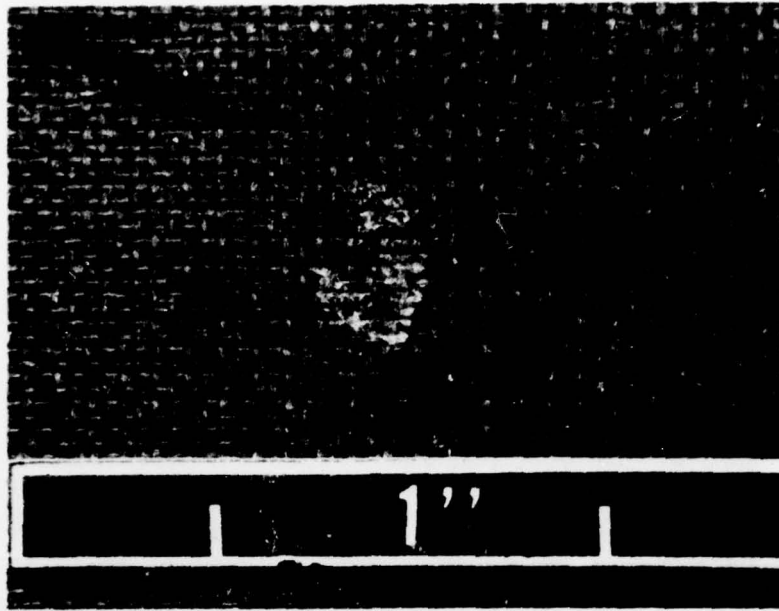
Front Face
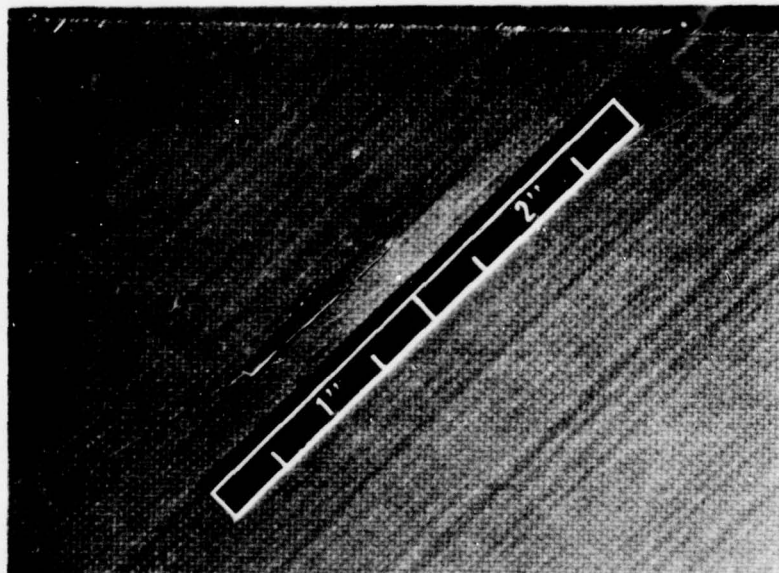
Back Face

Specimen ISP-8

Figure 4-1c. Typical Runway Stone Damage for 12 Ply G/E; Above Threshold
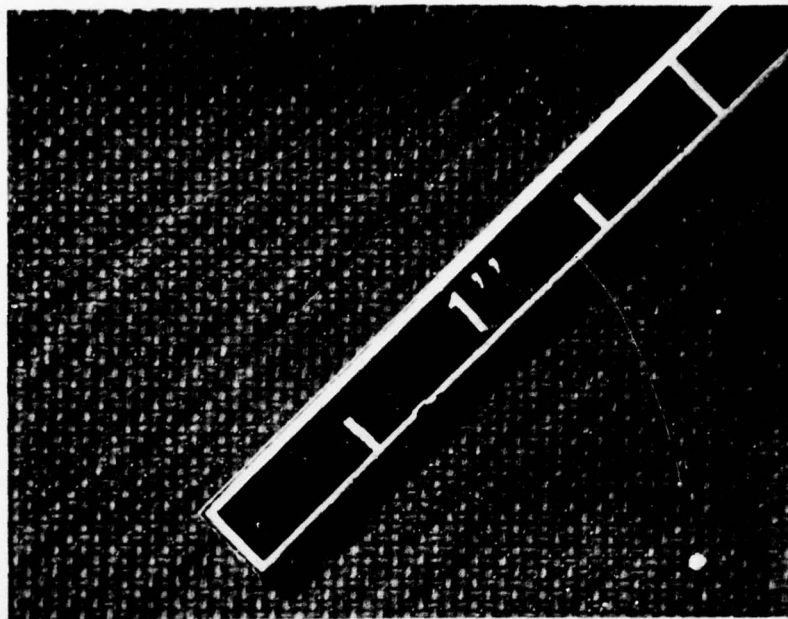
Specimen ISP-74a; R = 0.63cm (1/4-inch) Blunt Penetrator
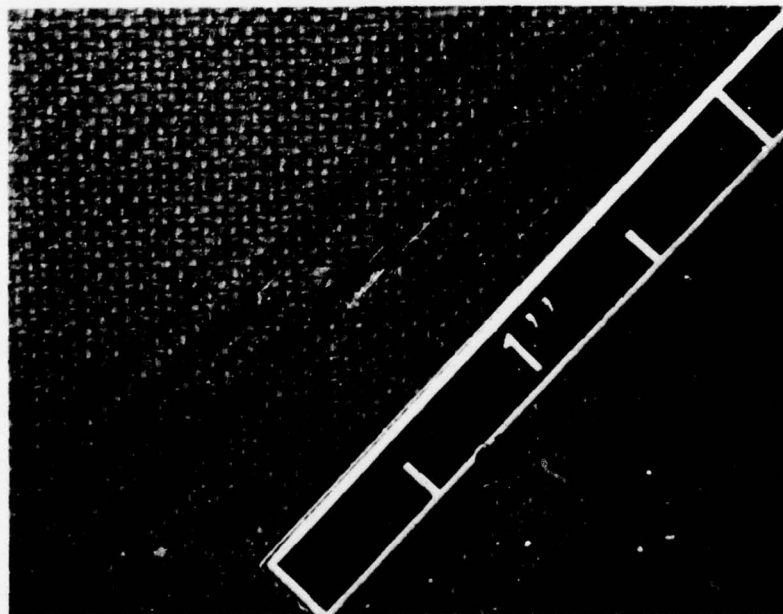
Specimen ISP-74a; R = 2.54cm (1-inch) Blunt Penetrator

Figure 4-2. Typical Above Threshold Backface Damage for Blunt
Penetrators; 12 Ply G/E Laminate
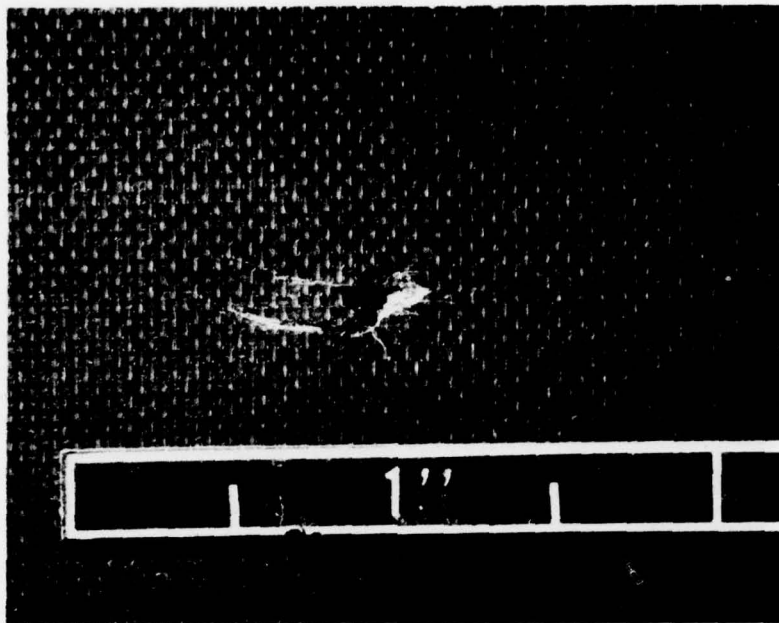
Specimen HCP-27; Runway Stone Impact
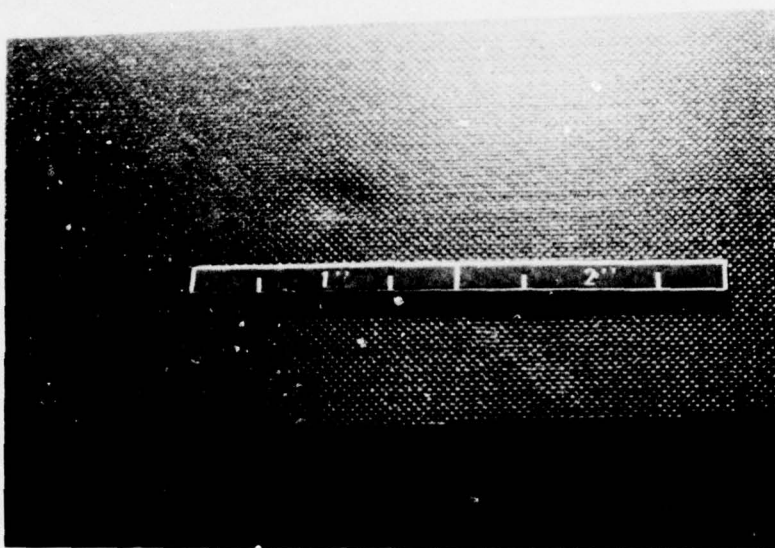
Specimen HCP-54; R = 0.63cm (1/4-inch) Blunt Penetrator

Figure 4-3a. Typical Above Threshold Damage; G/E Honeycomb Panels
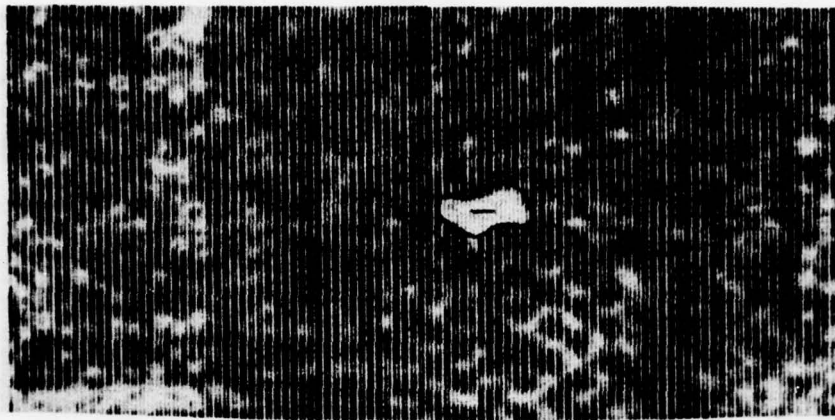
Specimen HCP-27; Runway Stone Impact
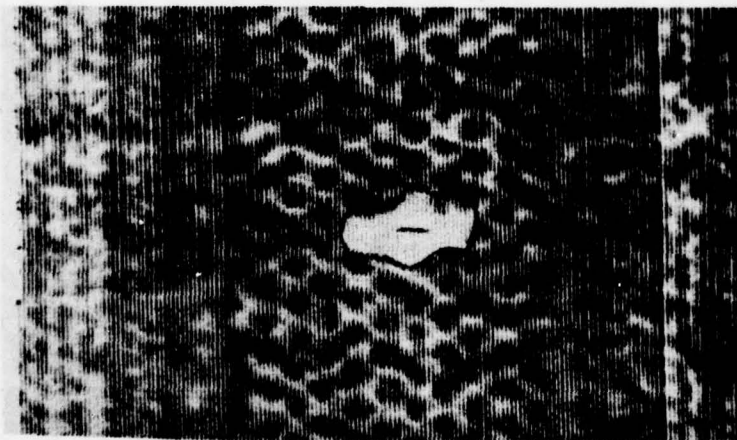
Specimen NCP-54; R = 0.63cm (1/4 inch) Blunt Penetrator

Figure 4-3b. C-Scans Corresponding to the Visual in Figure 4-3a

Table 4-3. Impact and Residual Tension Strength Data for Honeycomb Panels

Spec. No.	Threat Parameters			Ult Load (lb)	(N)	Percent Retention[1]	$\frac{mv^2}{2}$ ft-lb	J	Modulus of Elasticity ($\times 10^6$ psi)	
1	RS	m = 0.45gm	v = 53.6 m/s	1580	7027	90	0.476	0.646		
4			71.6	1035	4603	59	0.85	1.15	8.7	
7			93.3	885	3936	51	1.44	1.92		
10		m = 0.90gm	v = 40.5	1340	5960	77	0.54	0.738		
13			53.9	1036	4608	59	0.96	1.31	8.9	
16			70.1	963	4283	55	1.63	2.21		
19		m = 1.50gm	v = 29.3	1590	7072	91	0.472	0.641	9.3	
22			39.0	1050	4670	60	0.88	1.19	8.9	
25			50.6	968	4305	55	1.41	1.92	8.2	
28	R = 0.63cm	h = 1.22m	m = 81.0gm	1660	7383	95*	0.71	0.96		
31			108.0	1660	7383	95	0.94	1.28	8.8	
34		4.88m/s	140.4	1500	6672	86	1.23	1.67		
37		h = 2.74m	m = 53.3	1497	6658	86	1.06	1.43		
40			71.0	1010	4492	58	1.41	1.91	8.6	
43		7.35m/s	92.3	800	3558	46	1.83	2.48		
46		h = 6.1m	m = 28.5	1560	6939	87*?	1.26	1.70		
49			38.0	1012	4501	58	1.67	2.27	8.8	
52		10.9m/s	49.4	950	4225	54	2.18	2.95		
55	R = 2.54cm	h = 1.22m	m = 119.3	1760	7828	101*	1.04	1.41		
58			159.0	1758	7819	100	1.39	1.89	8.8	
61			206.7	1478	6574	84	1.81	2.45		
64		h = 2.74m	m = 75.0	1812	8059	104*?	1.49	2.02		
67			100.0	1585	7050	91*?	1.99	2.69	8.9	
70			130.0	1408	6262	80	2.58	3.50		
73		h = 6.1m	m = 52.5	1665	7406	95*?	2.31	3.14	9.2	
76			70.0	1666	7410	95	3.08	4.18	8.9	
79			91.0	1506	6698	86	4.01	5.44	9.1	
X-2	Drilled Hole	1/16 in.	1.6mm	1235	5493	71				
X-3		1/8 in.	3.1mm	1010	4492	57				
X-4		1/4 in.	6.3mm	944	4199	54				
X-5		1/2 in.	12.6mm	691	3073	39				

[1] Control Specimen Data

*Failure not through impact site
?Indicates a questionable observation

	Ult Load		
Spec. No.	(lb)	(N)	
1-1	1578	7019	8.3
2-1	1790	7962	9.3
3-1	1882	8371	9.3
X-1	1740	7739	
Avg.	1750	7784	9.0

σ = 765 MPa (111 ksi)

4-10

...t and Residual Tension Strength Data for Honeycomb Panels

	Ult Load (lb)	(N)	Percent Retention[1]	$\frac{mv^2}{2}$ ft-lb	J	Modulus of Elasticity ($\times 10^6$ psi)	(GPa)	Strain to Failure ($\times 10^{-6}$)
3.6 m/s	1580	7027	90	0.476	0.646			
1.6	1035	4603	59	0.85	1.15	8.7	60.0	6381
3.3	885	3936	51	1.44	1.92			
0.5	1340	5960	77	0.54	0.738			
3.9	1036	4608	59	0.96	1.31	8.9	61.4	6955
0.1	963	4283	55	1.63	2.21			
9.3	1590	7072	91	0.472	0.641	9.3	64.1	10500
9.0	1050	4670	60	0.88	1.19	8.9	61.4	7350
0.6	968	4305	55	1.41	1.92	8.2	56.5	6600
1.0gm	1660	7383	95*	0.71	0.96			
08.0	1660	7383	95	0.94	1.28	8.8	60.7	11100
40.4	1500	6672	86	1.23	1.67			
53.3	1497	6658	86	1.06	1.43			
71.0	1010	4492	58	1.41	1.91	8.6	59.3	5750
2.3	800	3558	46	1.83	2.48			
8.5	1560	6939	87*?	1.26	1.70			
8.0	1012	4501	58	1.67	2.27	8.8	60.7	6800
9.4	950	4225	54	2.18	2.95			
9.3	1760	7828	101*	1.04	1.41			
9.0	1758	7819	100	1.39	1.89	8.8	60.7	10800
6.7	1478	6574	84	1.81	2.45			
75.0	1812	8059	104*?	1.49	2.02			
0.0	1585	7050	91*?	1.99	2.69	8.9	61.4	9814
0.0	1408	6262	80	2.58	3.50			
2.5	1665	7406	95*?	2.31	3.14	9.2	63.4	11700
0.0	1666	7410	95	3.08	4.18	8.9	61.4	12400
1.0	1506	6698	86	4.01	5.44	9.1	62.7	10400
1.6mm	1235	5493	71					
3.1mm	1010	4492	57					
6.3mm	944	4199	54					
2.6mm	691	3073	39					

Spec. No.	Ult Load (lb)	(N)			
1-1	1578	7019	8.3	57.2	12700
2-1	1790	7962	9.3	64.1	12000
3-1	1882	8371	9.3	64.1	13000
X-1	1740	7739			
Avg.	1750	7784	9.0	61.8	12700

σ = 765 MPa (111 ksi)

Table 4-4. Impact and Residual Compression Strength Data for Honeycomb

Spec. No.	Threat Parameters			Ult Load* (lb)	(N)	Percent Retention[1]	$\frac{mv^2}{2}$ ft-lb	J	Modul (×10⁶)
2	RS	m = 0.45gm	v = 53.6 m/s	1403	6240	68	0.476	0.646	
5			71.6	924	4190	45	0.85	1.15	
8			93.3	1095	4870	53	1.44	1.92	9.8
11		m = 0.90gm	v = 40.5	1075	4781	52	0.54	0.738	
14			53.9	921	4096	45	0.96	1.31	
17			70.1	880	3914	43	1.63	2.21	9.2
20		m = 1.50gm	v = 29.3	1345	5982	65	0.472	0.641	10.0
23			39.0	1085	4826	52	0.88	1.19	10.0
26			50.6	1000	4480	48	1.41	1.92	10.0
29	R = 0.63cm	h = 1.22m	m = 81.0gm	1134	5044	55	0.71	0.96	
32			108.0	1144	5088	55	0.94	1.28	
35		4.88m/s	140.4	1020	4536	49	1.23	1.67	10.0
38		h = 2.74m	53.3	1038	4617	50	1.06	1.43	
41			71.0	942	4190	46	1.41	1.91	
44		7.35m/s	92.3	800	3558	39	1.83	2.48	8.9
47		h = 6.1m	m = 28.5	1076	4786	52	1.26	1.70	
50			38.0	1054	4688	51	1.67	2.27	
53		10.9m/s	49.4	720	3202	35	2.18	2.95	8.5
56	R = 2.54cm	h = 1.22m	m = 110.3gm	1596	7099	77	1.04	1.41	
59			159.0	1407	6258	68	1.39	1.89	
62		4.88m/s	206.7	1200	5337	58	1.81	2.45	9.9
65		h = 2.74m	m = 75.0	1352	6013	65	1.49	2.02	
68			100.0	880	3914	43	1.99	2.69	
71		7.35m/s	130.0	1060	4715	51	2.58	3.50	8.9
74		h = 6.1m	m = 52.5	890	3958	43	2.31	3.14	9.4
77		10.9m/s	70.0	830	3691	40	3.08	4.18	9.5
80			91.0	800	3558	39	4.01	5.44	10.2

[1] Control Specimen Data:

Spec No.	Ult Load (lb)	(N)		
5-1	2120	9429		9.7
6-1	2010	8940		8.9
7-1	2070	9207		9.5
Avg	2067	9194	σ = 951 MPa (138 ksi)	9.4

*All failures through impact site

	Ult Load* (lb)	(N)	Percent Retention[1]	$\frac{mv^2}{2}$ ft-lb	J	Modulus of Elasticity ($\times 10^6$ psi)	(GPa)	Strain to Failure ($\times 10^{-6}$)
53.6 m/s	1403	6240	68	0.476	0.646			
71.6	924	4190	45	0.85	1.15			
93.3	1095	4870	53	1.44	1.92	9.8	67.6	10900
40.5	1075	4781	52	0.54	0.738			
53.9	921	4096	45	0.96	1.31			
70.1	880	3914	43	1.63	2.21	9.2	63.4	6700
29.3	1345	5982	65	0.472	0.641	10.0	68.9	10000
39.0	1085	4826	52	0.88	1.19	10.0	68.9	8700
50.6	1000	4480	48	1.41	1.92	10.0	68.9	7400
81.0gm	1134	5044	55	0.71	0.96			
108.0	1144	5088	55	0.94	1.28			
140.4	1020	4536	49	1.23	1.67	10.0	68.9	5600
53.3	1038	4617	50	1.06	1.43			
71.0	942	4190	46	1.41	1.91			
92.3	800	3558	39	1.83	2.48	8.9	61.4	9600
28.5	1076	4786	52	1.26	1.70			
38.0	1054	4688	51	1.67	2.27			
49.4	720	3202	35	2.18	2.95	8.5	58.6	7900
10.3gm	1596	7099	77	1.04	1.41			
59.0	1407	6258	68	1.39	1.89			
06.7	1200	5337	58	1.81	2.45	9.9	68.3	10500
75.0	1352	6013	65	1.49	2.02			
100.0	880	3914	43	1.99	2.69			
30.0	1060	4715	51	2.58	3.50	8.9	61.4	19000
52.5	890	3958	43	2.31	3.14	9.4	64.8	7700
70.0	830	3691	40	3.08	4.18	9.5	65.5	11100
91.0	800	3558	39	4.01	5.44	10.2	70.3	3800

Load (lb)	(N)							
120	9429					9.7	66.9	15800
010	8940					8.9	61.4	15400
070	9207					9.5	65.5	16300
067	9194	σ = 951 MPa (138 ksi)				9.4	64.6	15800
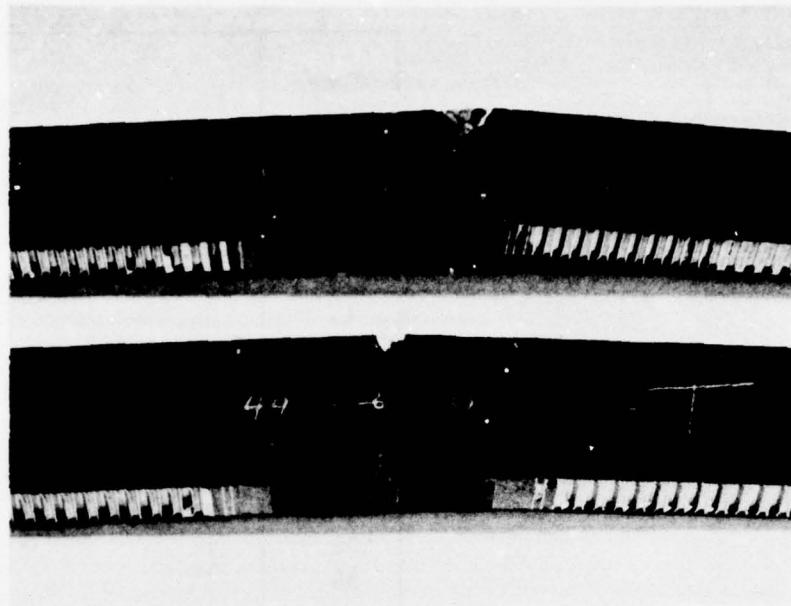
Figure 4-4. Typical Four Point Bend Sandwich Beam Tension
Specimens; Control and Damaged
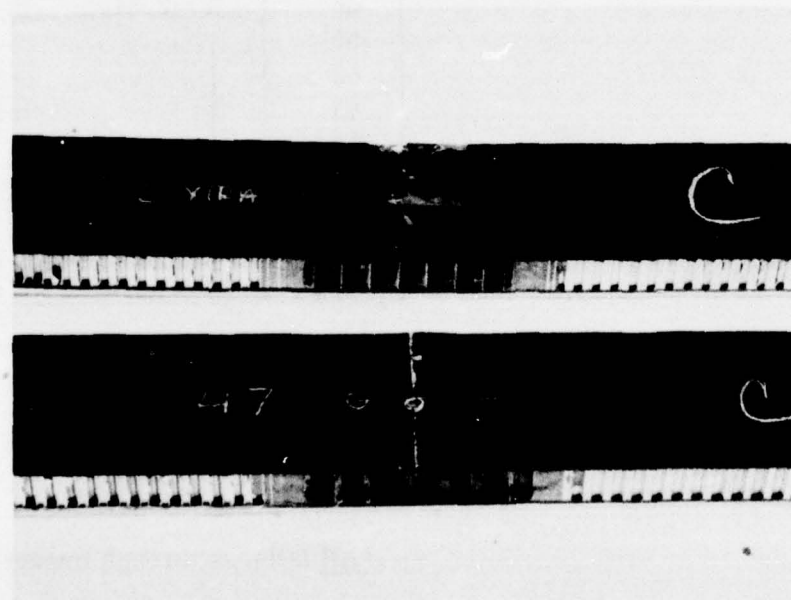
Figure 4-5. Typical Four Point Bend Sandwich Beam Compres-
sion Specimens; Control and Damaged

In each case a control specimen and a specimen containing a damage site has been included. As noted in the tables, all failures for the compression tests occurred through the impact damamge sites. For the tension specimens all but six specimens failed through the damage site. Four of these six failures occurred near the damage site, away from the potting. It is uncertain whether the damage site triggered catastrophic failure. The six specimen that failed at points other than through the damage site had percent retention strengths greater than 87%. The percent retention strength is merely the ratio of the ultimate load achieved by the damage specimen divided by the ultimate average load of the three control specimens.

A summary of the fatigue test results of the honeycomb test specimens is presented in Table 4-5. Several different specimens were used before the final configuration was found. The failures that were in the core or at the end are not considered acceptable.

Summaries of the residual tension strength and the crippling stress of the specimens from the stiffened panels are given in Tables 4-6 and 4-7. Several of the tensile failures were not at the damage location, but the values are consistent with the data from specimens that did fail through the damage. The compression tests all failed by crippling in modes that were considered acceptable.

The final set of data is the fatigue tests of the specimens from the I-stiffened panels. As with the HCP fatigue tests, some difficulties were experienced in the test method before settling on the R = +0.1 tests (tension-tension). The data is summarized in Table 4-8.

Table 4-5.   Fatigue Test Results of HCP Specimens

Spec No	Type of Damage	Type of Test	R Value	Max Load (lb)	Max Load (N)	Cycle to Failure	Type of Failure
3	RS	10-in. beam R	-0.9	1114	4955	12,860	shear of core
6		10-in. beam R	-0.9	1114	4955	5,557	in damage
9		10-in. beam	-0.9	1485	6600	9,723	shear
12		10-in. beam	-0.9	1485	6600	11,442	shear
15		10-in. beam R	-0.9	1114	4955	116,540	shear of core
18		10-in. beam R	-0.9	1114	4955	13,594	in damage
21		10-in. beam	-0.9	1114	4955	53,690+	
24		10-in. beam doubler	-0.9	1485	6600	1,614	shear
27		tensile		8686	38635	1,170	at the end
30	0.63cm	10-in. beam R	-0.9	1114	4955	59,596+	
33		10-in. beam R	-0.9	1114	4955	32,720	in damage
36		10-in. beam R	-0.9	1114	4955	5,061	in damage
39		10-in. beam	-0.9	1485	6600	15,325	shear
42		10-in. beam R	-0.9	1114	4955	83,448+	
45		10-in. beam R	-0.9	1114	4955	5,244	in damage
48		10-in. beam R	-0.9	1114	4955	30,637	shear of core
51		10-in. beam R	-0.9	1114	4955	11,912	in damage
54		10-in. beam R	-0.9	1114	4955	3,100	in damage
57	2.54cm						
60		10-in. beam R.	-0.9	1114	4955	55,647	core shear
63		10-in. beam R	-0.9	1114	4955	50,150+	
66		10-in. beam R	-0.9	1114	4955	34,900	core shear
69		10-in. beam R	-0.9	1114	4955	6,141	in damage
72		10-in. beam R	-0.9	1114	4955	39,553	in damage
75		10-in. beam	-0.9	1485	6600	8,484	shear
78		10-in. beam R		1114	4955	118	in damage
81		10-in. beam R	-0.9	1114	4955	38,300	in damage
Control		9-in. beam	-0.9	1733	7708	1,652	core shear
8-1		10-in. beam doubler	-0.9	1485	6600	1,556	shear
4-1		10-in. beam	-0.9	1485	6600	7,753	shear

Types of specimen

tensile - original design to load the beams in tension

10-in. beam doubler - 4 pt bending beam with a .254m (10-in.) span but with the aluminum doublers from the tensile left on

9-in. beam - 4 pt. bending beam with a .228m (9-in.) span

10-in. beam R - 4 pt bending beam with a .254m (10-in.) span and a reduced center section

Table 4-6. Impact and Residual Compression Strength for I-Stiffene[s]

Spec. No.	Threat Parameters			Ult Load (lb)	(N)	Percent Retention [1]	$\frac{mv^2}{2}$ ft-lb	J
2	RS	m = 0.45 gm	v = 88.1 m/s	4700	20905	101	1.28	1.74
5			103	4550	20238	98	2.28	3.09
8			153	3735	16613	80	3.88	5.25
11		m = 0.90 gm	v = 66.4	4650	20683	100	1.46	1.98
14			88.4	4460	19838	96	2.59	3.51
17			115	4630	20594	100	4.37	1.36
20		m = 1.50 gm	v = 47.8	4945	21995	106	1.26	1.71
23			64.0	4835	21506	104	2.26	3.07
26			82.9	4800	21350	103	3.79	5.14
29	R = 0.63cm	h = 1.22m	m = 108 gm	4355	19371	94	0.95	1.28
32		4.87m/s	140.4	4700	20905	101	1.23	1.67
35			182.5	4740	21083	109	1.60	2.16
38		h = 2.74m	m = 71	4765	21194	102	1.41	1.91
41		7.34m/s	92.3	4740	21083	102	1.83	2.48
44			120	4700	20905	101	2.38	3.23
47		h = 6.09m	m = 38	4875	21684	105	1.67	2.27
50		10.9m/s	49.4	5315	23641	114	2.18	2.95
53			64.2	5160	22951	111	2.83	3.83
56	R = 2.54cm	h = 1.22m	m = 159 gm	4840	21528	104	1.39	1.89
59		4.87m/s	206.7	4575	20349	98	1.81	2.45
62			268.7	4610	20505	99	2.35	3.19
65		h = 2.74m	m = 100	4750	21128	102	1.99	2.69
68		7.34m/s	130	4645	20660	100	2.58	3.50
71			169	4755	21150	102	3.36	4.55
74		h = 6.09m	m = 70	5000	22240	107	3.09	4.18
77		10.9m/s	91	4455	19815	96	4.01	5.44
80			118.3	4700	20905	101	5.21	7.07

Control Specimen Data:	Spec. No.	Ult Load (lb)	(N)
	6-1	5130	22 818
	6-2	4600	20 460
	5-1	4230	18 815
	Avg.	4653	20 696

	Ult Load (lb)	(N)	Percent Retention[1]	$\frac{mv^2}{2}$ ft-lb	J	Modulus of Elasticity (x 10^6 psi)	(GPa)	Strain to Failure (x 10^{-6})
.1 m/s	4700	20905	101	1.28	1.74	8.3	57.2	2700
3	4550	20238	98	2.28	3.09			
3	3735	16613	80	3.88	5.25			
.4	4650	20683	100	1.46	1.98			
.4	4460	19838	96	2.59	3.51			
5	4630	20594	100	4.37	1.36			
.8	4945	21995	106	1.26	1.71			
.0	4835	21506	104	2.26	3.07			
.9	4800	21350	103	3.79	5.14	8.1	55.8	3100
8 gm	4355	19371	94	0.95	1.28	8.5	58.6	2800
0.4	4700	20905	101	1.23	1.67			
2.5	4740	21083	109	1.60	2.16			
1	4765	21194	102	1.41	1.91			
.3	4740	21083	102	1.83	2.48			
0	4700	20905	101	2.38	3.23			
8	4875	21684	105	1.67	2.27	8.2	56.5	3000
9.4	5315	23641	114	2.18	2.95			
4.2	5160	22951	111	2.83	3.83			
9 gm	4840	21528	104	1.39	1.89			
6.7	4575	20349	98	1.81	2.45			
8.7	4610	20505	99	2.35	3.19			
0	4750	21128	102	1.99	2.69			
0	4645	20660	100	2.58	3.50			
9	4755	21150	102	3.36	4.55			
0	5000	22240	107	3.09	4.18	7.6	52.4	3600
1	4455	19815	96	4.01	5.44			
8.3	4700	20905	101	5.21	7.07	8.5	58.6	3000

c. No.	Ult Load (lb)	(N)						
-1	5130	22 818				8.3	57.2	3500
-2	4600	20 460				8.3	57.2	3000
-1	4230	18 815				8.3	57.2	1600
Avg.	4653	20 696				8.3	57.2	2700

4-15

Spec. No.	Threat Parameters			Load (lb)	(N)	Percent Retention [1]	$\frac{mv^2}{2}$ ft-lb	J	Modulu (x 10^6
1	RS	m = 0.45 gm	v = 881 m/s	11950	53153	97	1.28	1.74	7.8
4			103	9650	42923	78	2.28	3.09	
7			153	6300	28022	51	3.88	5.25	
10		m = 0.90 gm	v = 66.4	10000	44480	81	1.46	1.98	
13			88.4	6300	28022	51	2.59	3.51	
16			115	7050	31358	57	4.37	1.36	
19		m = 1.50 gm	v = 47.8	10300	45814	84	1.26	1.71	
22			64.0	10500	46704	85	2.26	3.07	7.6
25			82.9	6250	27800	51	3.79	5.14	
28	R = 0.63 cm	h = 1.22 m	m = 108 gm	11300	50262	92	0.95	1.28	
31		4.87 m/s	140.4	13100	58268	107	1.23	1.67	
34			182.5	10300	45814	84	1.60	2.16	
37		h = 2.74 m	m = 71	9780	43501	80	1.41	1.91	7.6
40		7.34 m/s	92.3	11150	49595	91	1.83	2.48	
43			120	10000	44480	81	2.38	3.23	
46		h = 6.09 m	m = 38	10900	48483	89	1.67	2.27	
49		10.9 m/s	49.4	10800	48038	88	2.18	2.95	
52			64.2	8800	39142	72	2.83	3.83	7.6
55	R = 2.54 cm	h = 1.22 m	m = 159 gm	12000	53376	98	1.39	1.89	7.9
58		4.87 m/s	206.7	10800	48038	88	1.81	2.45	
61			268.7	11000	48928	89	2.35	3.19	
64		h = 2.74 m	m = 100	11500	51152	93	1.99	2.69	
67		7.34 m/s	130	11400	50707	93	2.58	3.50	
70			169	11000	48978	89	3.36	4.55	
73		h = 6.09 m	m = 70	8250	36696	67	3.09	4.18	
76		10.9 m/s	91	10500	46704	85	4.01	5.44	
79			118.3	11735	52197	95	5.21	7.07	7.7

Control Specimen Data:	Spec. No.	Ult Load (lb)	(N)	(MPa)	
	2-3 5.0cm (2 in.) wide	12,300	54710	650	
	1 2.5cm (1 in.) wide	6,950	30913	659	8.1
	2 2.5cm (1 in.) wide	6,900	30691	678	8.1
	4 2.5cm (1 in.) wide	6,730	29935	662	8.0
	5 2.5cm (1 in.) wide	6,775	30135	671	8.0
	Avg.		664		8.0

	Load (lb)	(N)	Percent Retention [1]	$\frac{mv^2}{2}$ ft-lb	J	Modulus of Elasticity (x 10^6 psi)	(GPa)	Strain to Failure (x 10^{-6})
= 881 m/s	11950	53153	97	1.28	1.74	7.8	53.8	11800
103	9650	42923	78	2.28	3.09			
153	6300	28022	51	3.88	5.25			
= 66.4	10000	44480	81	1.46	1.98			
88.4	6300	28022	51	2.59	3.51			
115	7050	31358	57	4.37	1.36			
= 47.8	10300	45814	84	1.26	1.71			
64.0	10500	46704	85	2.26	3.07	7.6	52.4	10500
82.9	6250	27800	51	3.79	5.14			
= 108 gm	11300	50262	92	0.95	1.28			
140.4	13100	58268	107	1.23	1.67			
182.5	10300	45814	84	1.60	2.16			
= 71	9780	43501	80	1.41	1.91	7.6	52.4	9640
92.3	11150	49595	91	1.83	2.48			
120	10000	44480	81	2.38	3.23			
= 38	10900	48483	89	1.67	2.27			
49.4	10800	48038	88	2.18	2.95			
64.2	8800	39142	72	2.83	3.83	7.6	52.4	8630
= 159 gm	12000	53376	98	1.39	1.89	7.9	54.5	11450
206.7	10800	48038	88	1.81	2.45			
268.7	11000	48928	89	2.35	3.19			
= 100	11500	51152	93	1.99	2.69			
130	11400	50707	93	2.58	3.50			
169	11000	48978	89	3.36	4.55			
= 70	8250	36696	67	3.09	4.18			
91	10500	46704	85	4.01	5.44			
118.3	11735	52197	95	5.21	7.07	7.7	53.1	11300

Spec. No.	Ult Load (lb)	(N)	(MPa)	(x 10^6 psi)	(GPa)	Strain to Failure (x 10^{-6})
5.0cm (2 in.) wide	12,300	54710	650			
2.5cm (1 in.) wide	6,950	30913	659	8.1	55.8	11800
2.5cm (1 in.) wide	6,900	30691	678	8.1	55.8	12200
2.5cm (1 in.) wide	6,730	29935	662	8.0	55.2	12000
2.5cm (1 in.) wide	6,775	30135	671	8.0	55.2	12200
Avg.			664	8.0	55.4	12000

Table 4-8. Fatigue Test Results from I-Stiffened Panel Specimens

Spec No.	Type of Damage	R Value	Cycles to Failure	Type of Failure lb		N
3	RS	+0.1	2,520,000+	Tensile	12,150	54 043
6		+0.1	2,500,000+		10,820	48 127
9		-0.4	174,000	At doubler		
12		+0.1	2,110,000	In grip		
15		+0.1	2,546,000+	Tensile	10,300	45 814
18		-0.4	163,000	At doubler		
21		+0.1	5,300,000+	Tensile	11,430	50 840
24		+0.1	2,535,000+		9,350	41 588
27		-0.4	2,005,000	In test section		
30	0.63cm	+0.1	2,597,000+	Tensile	13,000	57 824
33		+0.1	2,552,000+		12,000	53 376
36		-0.4	1,000	At doubler		
39		+0.1	2,529,000+	Tensile	8,120	36 117
42		+0.1	2,500,000+		9,700	43 145
45		+0.1	2,508,000+		10,230	45 503
48		+0.1	2,547,000+		12,400	55 155
51		+0.1	2,609,000+		12,000	53 376
54		+-.1	2,550,000+		11,000	48 928
57	2.54cm	+0.1	2,544,000+	Tensile	10,550	46 926
60		+0.1	2,590,000+		11,950	53 153
63		+0.1	2,502,000+		12,000	53 376
66		+0.1	2,560,000+		12,300	54 710
68		+0.1	2,563,000+		12,200	54 265
72		+0.1	2,500,000+		11,140	49 550
75		+0.1	2,573,000+		11,500	51 152
78		+0.1	2,500,000+		12,000	53 376
81		+0.1	2,531,000+		10,730	47 727
Control						
4-3		+0.1	2,507,000+	Tensile	10,550	46 926
4-1		-0.4	4,361,000+			

+Did not fail

Load = 25 020 N (5625 pounds)
σ = 298 MPa (43.3 ksi)

SECTION 5

ANALYSIS AND DESIGN IMPLICATION OF THE TEST DATA

5.1 DAMAGE

An immediate result is that it is possible to observe damage in the I-stiffened panels rather easily, but this damage tends to be more associated with the back face than the impacted face. A schematic of the position of all of the damage due to each type of impactor is shown in Figure 5-1. From the summary of the size of damage, one notes that the damage is much more extensive than can be visually observed.

The C-scan data are a true indication because they were run at relatively high gain. Under these conditions, total signal loss would not be expected unless a total disbond condition existed. At high gain, the disbond boundaries are slightly reduced. Therefore, actual disbonds may be slightly larger than the C-scan indications, but this error is normally no more than 2 to 3 mm. Detailed investigations on the screening panel tests has shown that when cross-sections were made, they conformed the C-scan results.

It is interesting to note that in every case extensive delamination-type damage seems to occur between the +45 and -45 plies. Based on these results it may prove advantageous to use woven fabric for the +45 and -45 plies in an attempt to interlock them and reduce the amount of delamination damage during impact. While this could potentially improve the damage characteristics of the material, it may only result in moving the major delaminations to the innerface between the unidirectional 0-degree plies and the ±45-degree woven fabric.

Two obvious factors come to mind with these results. First is what effect, if any, the position of the +45 and -45 plies has on the resistance to impacts. If the plies were all on the inside, would the damage tolerance be higher or lower. Second, if we have a total delamination, this is an excellent spot to trap moisture. In this program we dried all the specimens before testing, but there is ample data showing that moisture affects the mechanical properties. We do not know if this effect would be increased by the pre-existing damage.

The damage observed in the honeycomb panels was even more disturbing. The visual damage was extremely slight, and in fact with the one-inch penetrator there was no really definable visual damage. The subsequent C-scans of the panels did show substantial damage. This presents some real maintainability problems. A dropped wrench does not make a mark, but it does damage the aircraft structure. As will be shown later this does degrade the properties, and all with no visual evidence. The reason may well be that the damage is in core crushing. The phenolic core used in the program has wide application because it minimizes corrosion and is not an electrical conductor, but its poor impact resistance may well prove a more serious liability. Work needs to be done using a less brittle core such as aluminum.
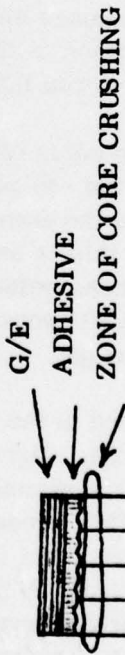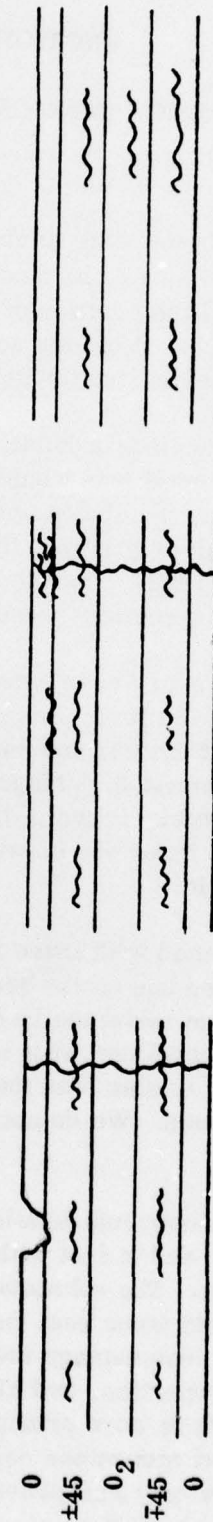
I-STIFFENED PANELS

RUNWAY STONES

SMALL BLUNT
R = 1/4 IN.

LARGE BLUNT
R = 1 IN.

±45
0₂
∓45
±45
0₂
∓45

HONEYCOMB PANELS

0
±45
0₂
∓45
0

G/E
ADHESIVE
ZONE OF CORE CRUSHING
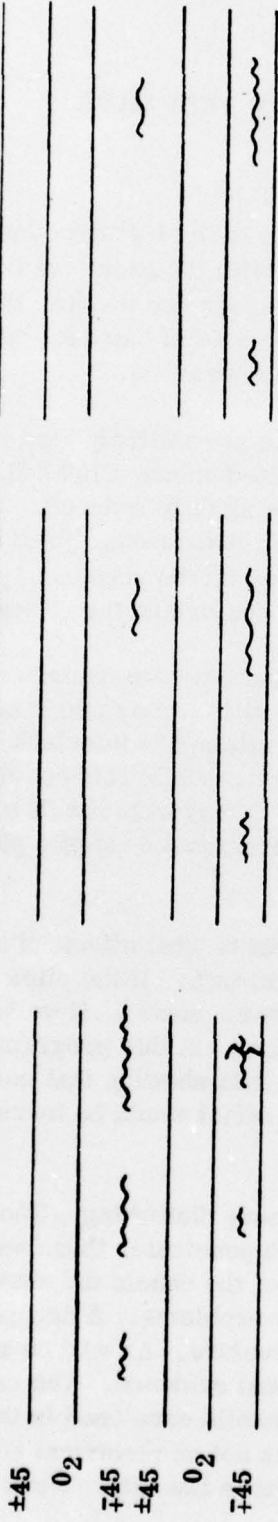
1-2 CELLS
CRUSHED

2-3 CELLS
CRUSHED

4-5 CELLS
CRUSHED

Figure 5-1. Progression of Impact Damage

Attempts have been made on both types of construction to correlate this measured damage to the physical parameters making the threat (mass, height, velocity, etc.) The data is very scattered, which makes it difficult to determine the best correlation. The trend that emerges is that the energy of the threat is most related to the size of the damage. Physically one can understand that the more energy imparted into a system the more that must be absorbed by the part, which leads to damage. One would also expect to see a threshold below which the system was able to absorb all imparted energy with no damage. The data shown in Figures 5-2 and 5-3 suggests that this interpretation is correct.

5.2 HONEYCOMB PANEL

The first objective of this program was to determine if visual threshold damage would cause any degradation of measured properties. The answer to this question is a dramatic yes as shown graphically in Figures 5-4 and 5-5. These data suggest that the strength of specimen from HCP are reduced up to 50% at visual threshold. The C-scans do show the damage but since an aircraft is only inspected periodically, one then has to design to take into account this degradation. To obtain a better understanding of this phenomena, four specimens with various size holes were tested. These data are plotted in Figure 5-6 and show a good correlation between the size of damage observed visually and the hole size specimens. This suggests that the design of a structure with this material must be such that it will withstand a 1/4-inch diameter hole (6.3mm), which could be drilled at any position.

The tensile strength of HCP specimen is degraded by the impacts in relation to the energy of the impact. The sharper the impactor the more localized the damage and the more the specimen behaves as a specimen with a hole. These trends are clearly shown in Figure 5-7. This obviously is a laminate (facesheet) behavior.

The compression data on the HCP specimens is different than the data on the flat panels. The compression strength is reduced in relation to the energy of the inducing damage regardless of the type of impact. The first factor is that the compression strength is reduced substantially in contrast to no reduction in the flat laminate. The reasoning may in fact be tied to the reasons postulated in the crippling results. In the flat laminate crippling test, the panel could buckle and move the load away from the damage over to the edge of the specimen. For honeycomb panel specimens, this buckling is prevented by the bonded core, and hence the center is fully loaded. The failure then becomes a compression failure.

This compression failure is probably due to the lack of support by the core rather than an inherent failure of the fibers. In reviewing the damage caused by the penetrators (Figure 5-8), it is obvious that they all cause damage of the core. It also seems obvious that this damage is directly related to the energy of the penetrator. It therefore seems reasonable that the failure strengths are all related to the energy of the penetrator. The data from the larger penetrator is slightly above the other data, but the major cause does seem to be due to the core damage.
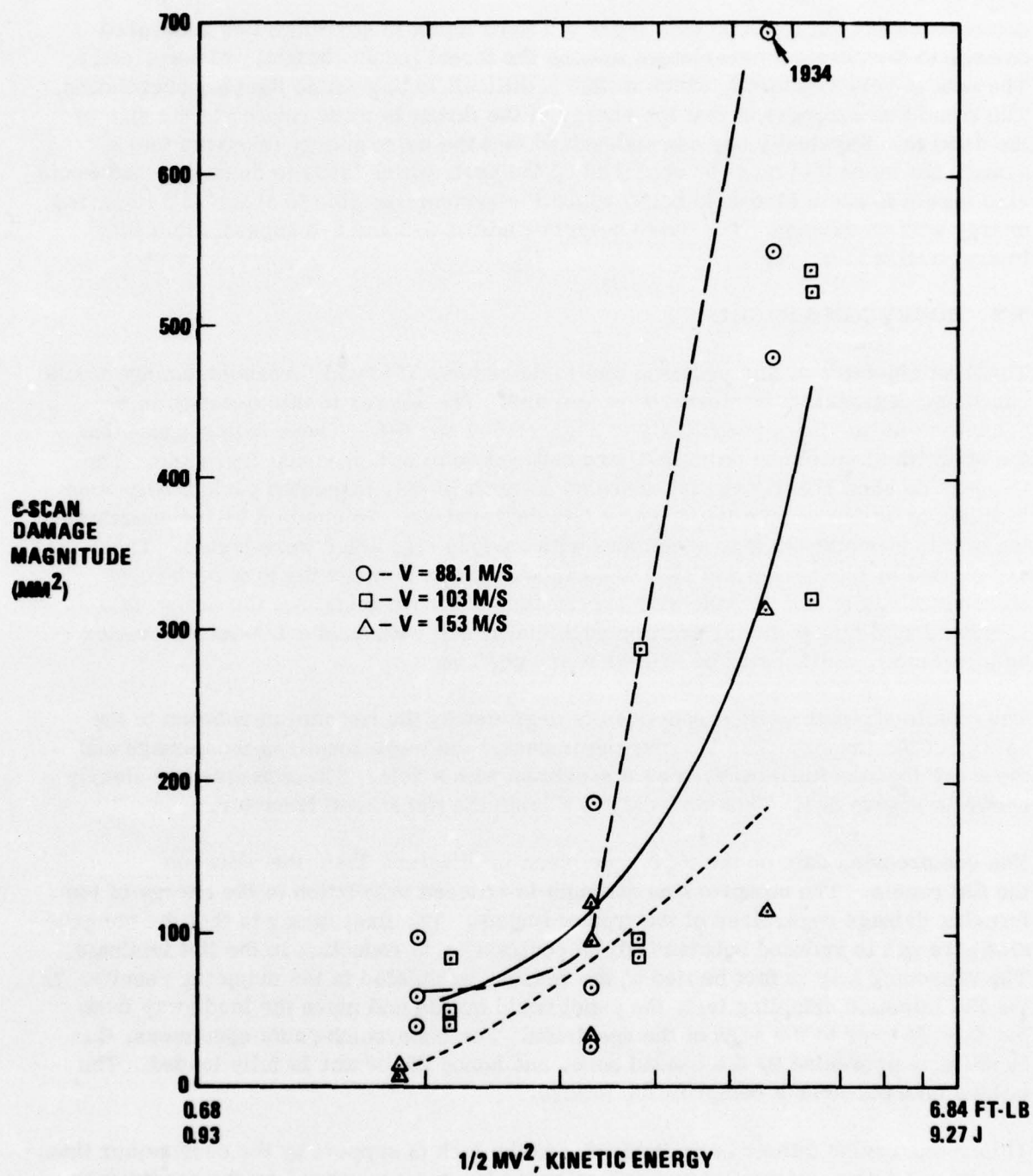
5-3

Figure 5-2. C-Scan-Detected Damage by Runway Stones to
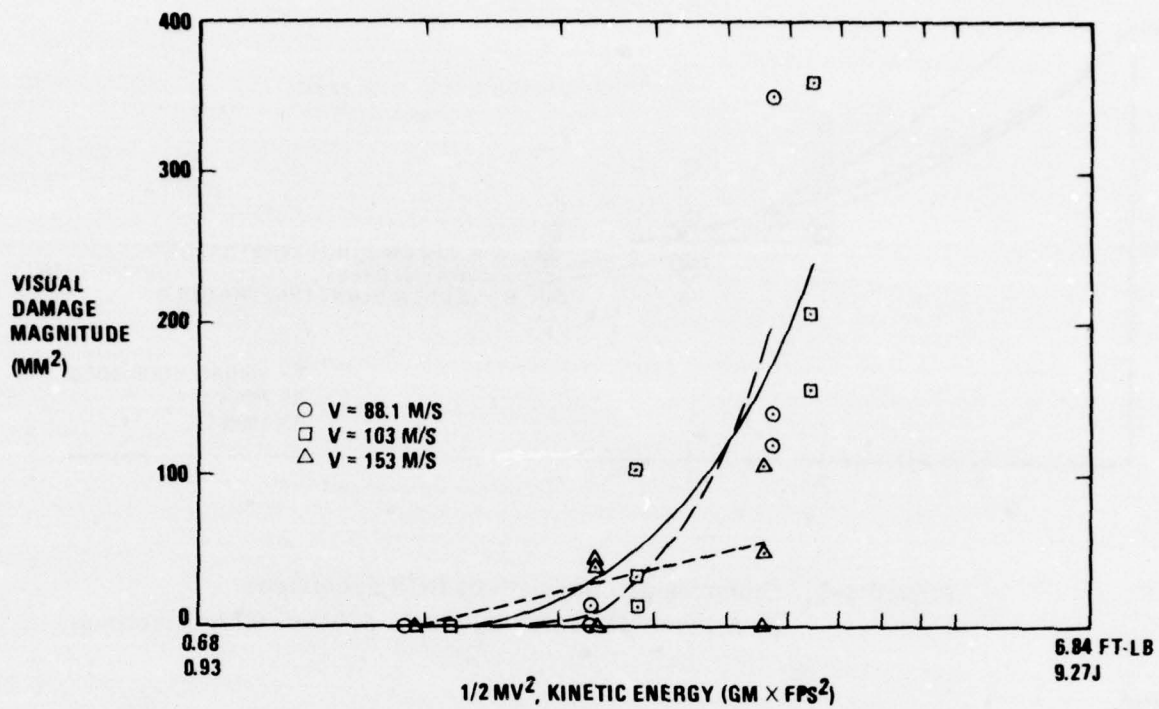I-Stiffened Panels

Figure 5-3. Visually Detected Damage by Runway Stones to I-Stiffened Panels
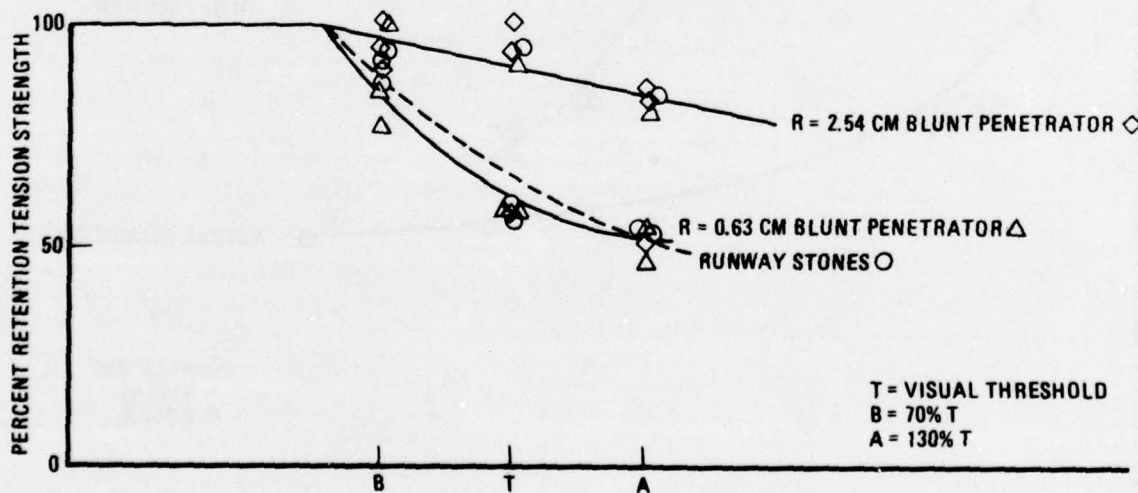
Figure 5-4. Tensile Strength of HCP Specimens
as a Function of Damage for 5.04cm
Wide Specimens

5-5

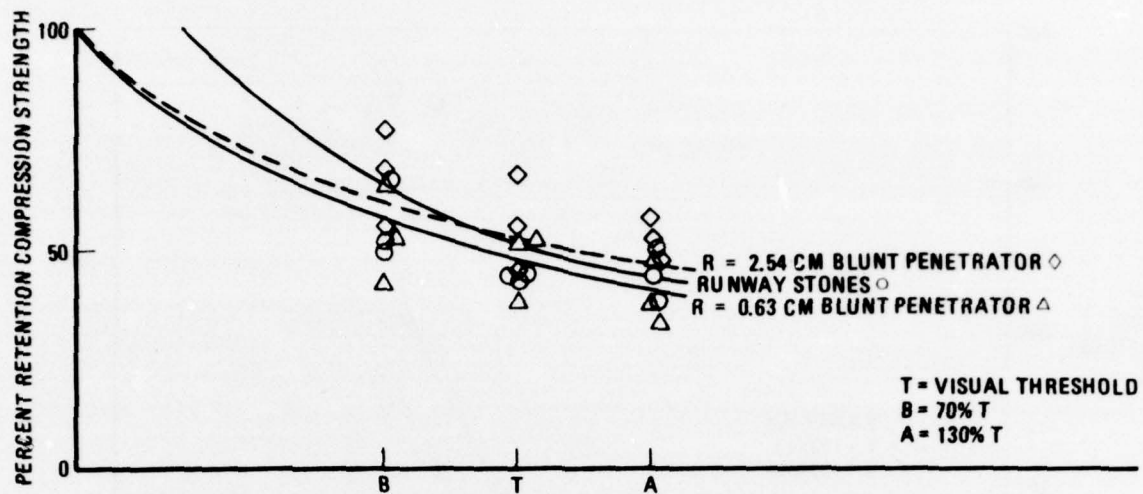Figure 5-5. Compression Strength of HCP Specimens
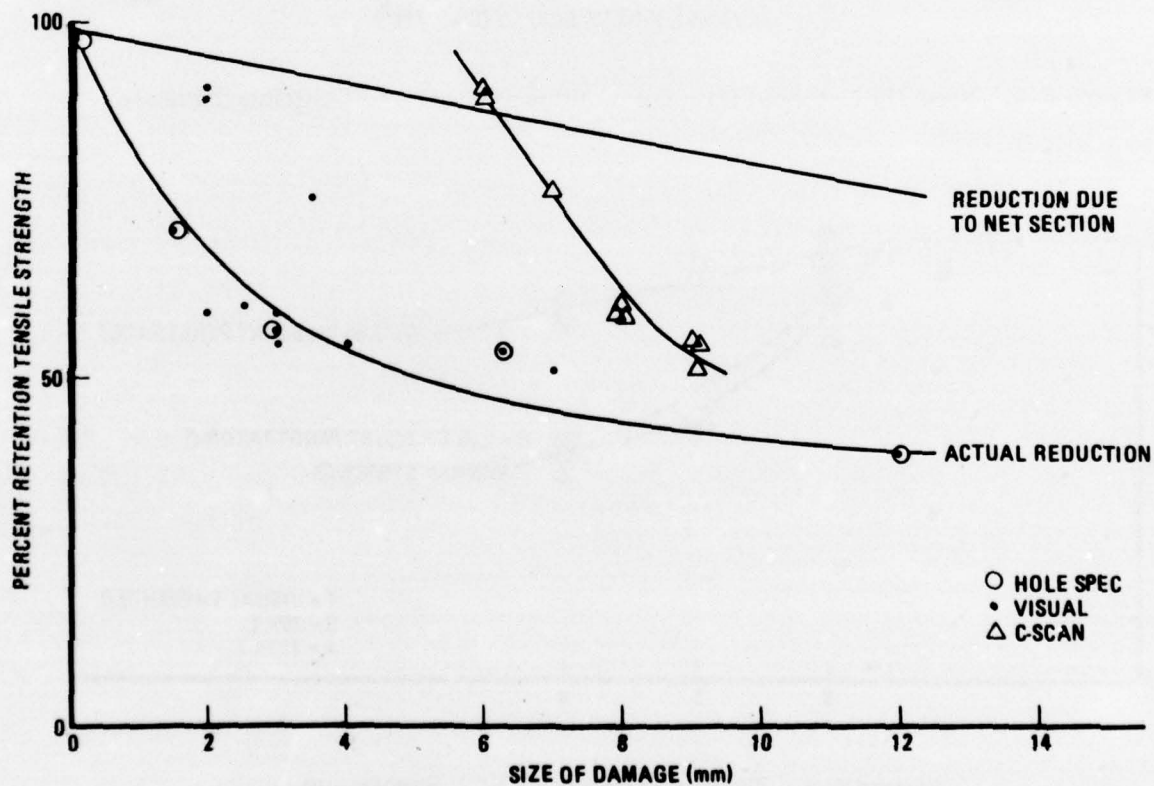as a Function of Damage for a 5.04cm Wide Specimen

Figure 5-6. Tensile Strength as a Function of Hole Size for HCP
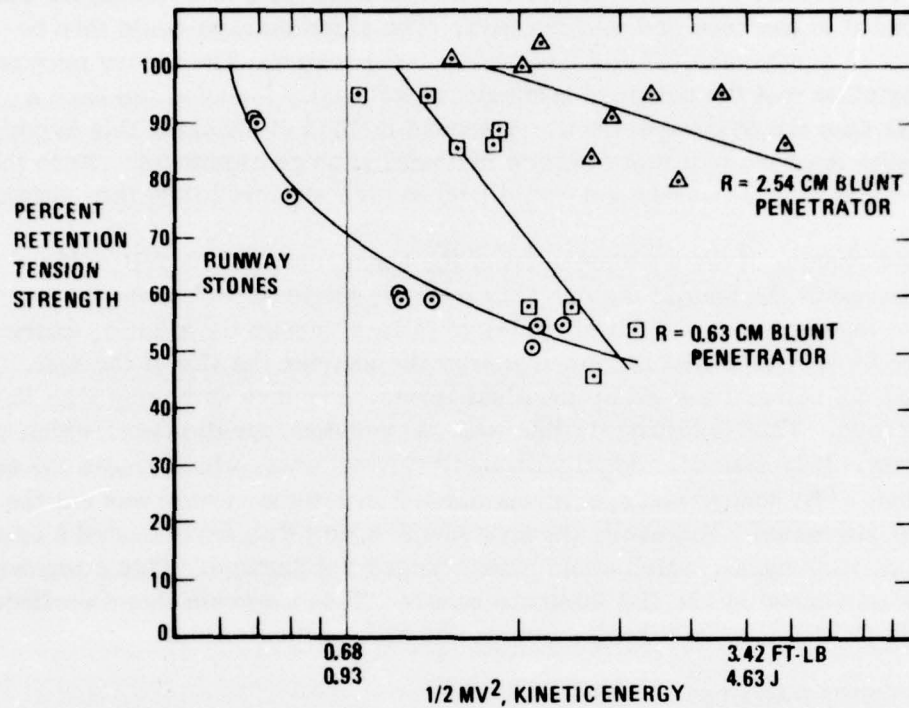Specimen Damage With Runway Stones

Figure 5-7. Percent Retention Tension Strength Versus Kinetic Energy
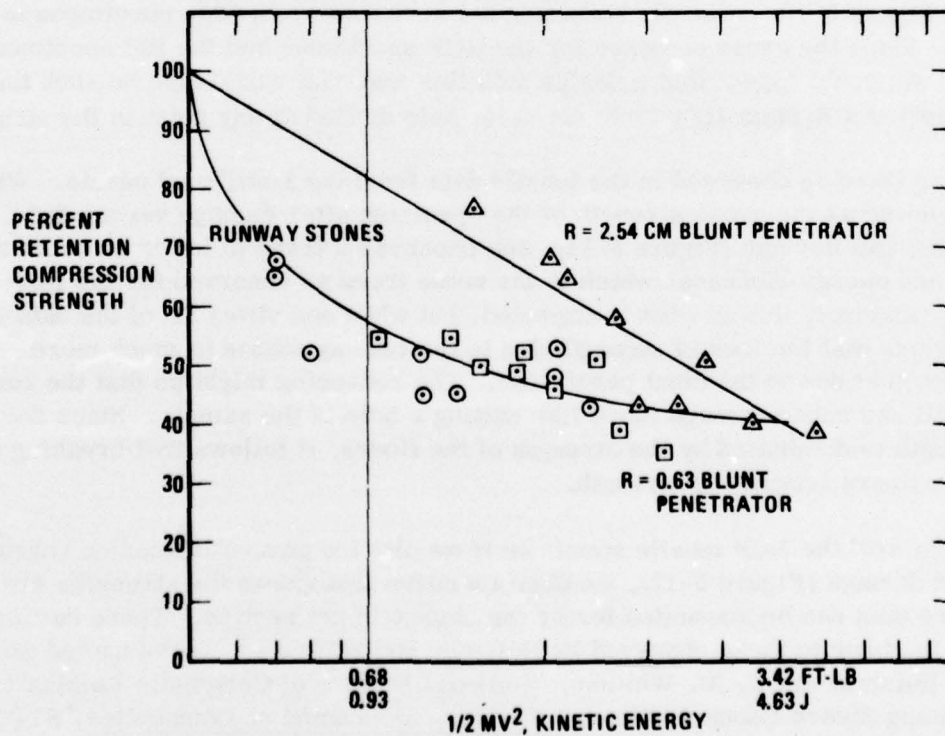at Impact; Honeycomb Panels

Figure 5-8. Percent Retention Compression Strength Versus Kinetic
Energy at Impact; Honeycomb Panels

Two methods of checking out this hypothesis are possible. One is to damage a laminate and then to bond it to the core and test the part. The same damage could then be induced in a boned honeycomb panel subsequently to be tested. The theory proposed here would postulate that the damaged laminate subsequently boned would have a higher strength than the other specimen. A second method of checking this hypothesis would be to make the core of a more elastic material such as aluminum. Here the core would not fragment as easily and would tend to give support to the face sheet.

The fatigue test results of the specimens from the honeycomb panels follow the same trends as observed in the tensile tests. This is as we might expect since the maximum load was in the tension face. A plot of cycles to failure versus the kinetic energy at impact (Figure 5-9) shows that the more energy the shorter the life of the test. It also shows that the damage caused by the blunt impactor is less damaging than the sharper impactors. This is clearly in line with the previous tensile data, which shows the same effects. It is also consistent with the flat panel data, which shows the same effect in tension. The honeycomb specimens did fail in fatigue, which was not the case of the flat laminates. However, the honeycomb specimens experienced a compression load on each cycle, which could have changed the damage. This compression load was not experienced by the flat laminate panels. This suggests that the effect of compression in fatigue may be a contributor to the failure mechanism.

5.3 I-STIFFENED PANELS

As with the HCP specimen, the objectives of this program was to determine if visual threshold damage would cause a degradation of properties. Again the answer is yes as shown in Figure 5-10. Also the reduction for 5.3cm (2-inch) wide specimens is approximately 50%. Since the gross stresses for the HCP specimens and the ISP specimens are similar, we could expect that a design with this material would also be such that it could withstand a 6.3mm (1/4-inch) diameter hole drilled at any point in the structure.

An interesting trend is observed in the tensile data from the I-stiffened panels. When the data is viewed as the gross strength of the specimen after damage versus the energy making that damage (Figure 5-11), one observes a trend to lower strength as the damage and energy increase, which is the same trend as observed for the HCP specimens. Obviously this is what is expected, but when one views all of the data it becomes obvious that the loss of strength due to the runway stones is much more extensive than that due to the blunt penetrator. The reasoning might go that the runway stone is small and cause damage more like cutting a hole in the sample. Since the tensile strength is dominated by the strength of the fibers, it follows that breaking or removing the fibers lowers the strength.

As in the case with the HCP tensile specimen if we plot the percent retension versus the observed damage (Figure 5-12), we obtain a curve that shows the strengths are reduced more than can be accounted for by the change in net section. These curves are similar in shape to those observed by Nuismer and Whitney.[3] In the quoted work,

3. R. J. Nuismer and J. M. Whitney, "Uniaxial Failure of Composite Laminates Containing Stress Concnetrations," Fracture Mechanics of Composites, STP 593 ASTM, 1974, Page 117.

100,000 PLUS

R = 2.54 CM

10,000

CYCLES TO
FAILURE

R = 0.63 CM

1,000

● RUNWAY STONE
■ 0.63 CM PENETRATOR
▲ 2.54 CM PENETRATOR
↑ NO FAILURE
⌐ CORE SHEAR

100

0.68   3.42 FT-LB
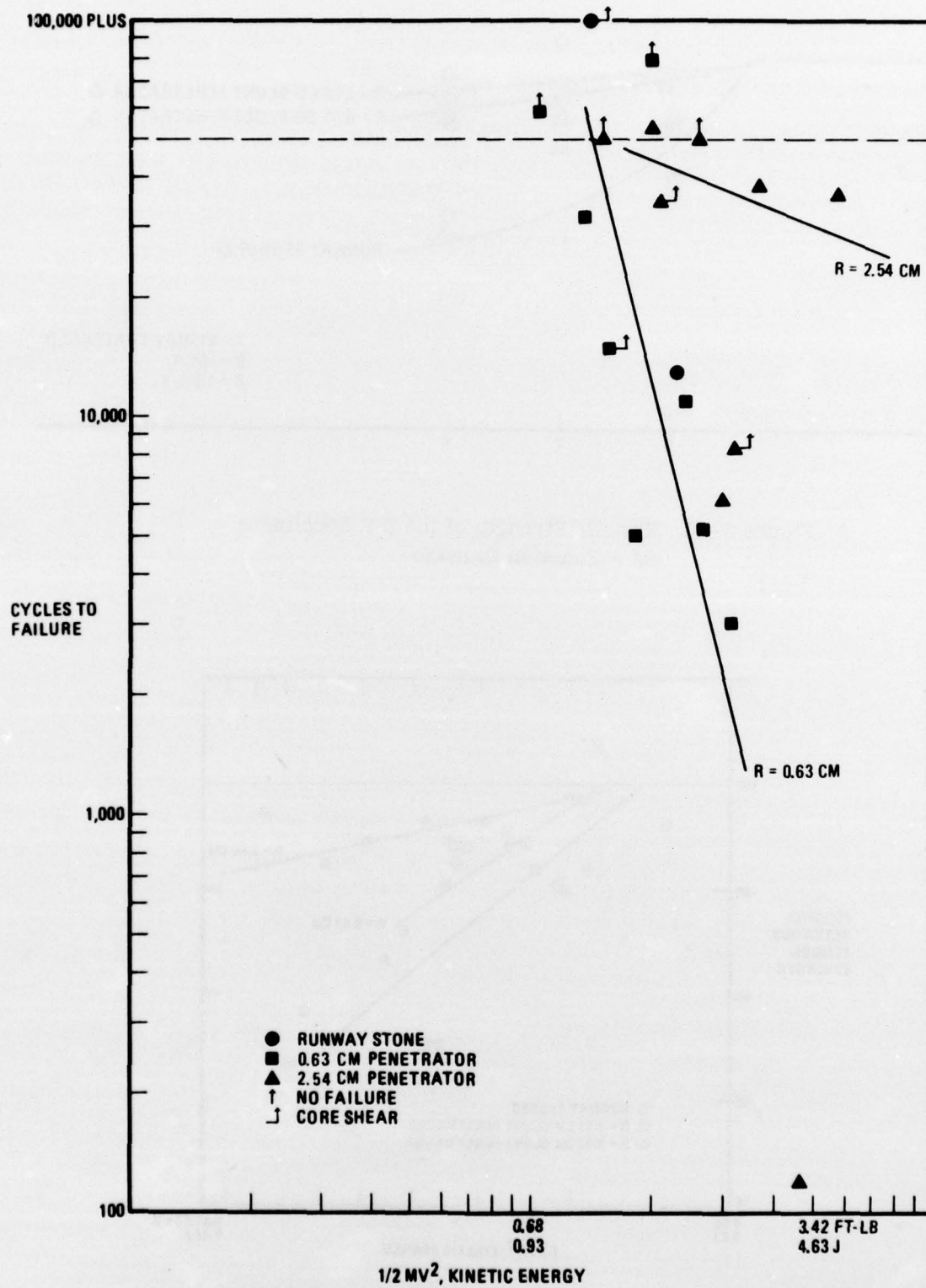0.93   4.63 J

$1/2\ MV^2$, KINETIC ENERGY

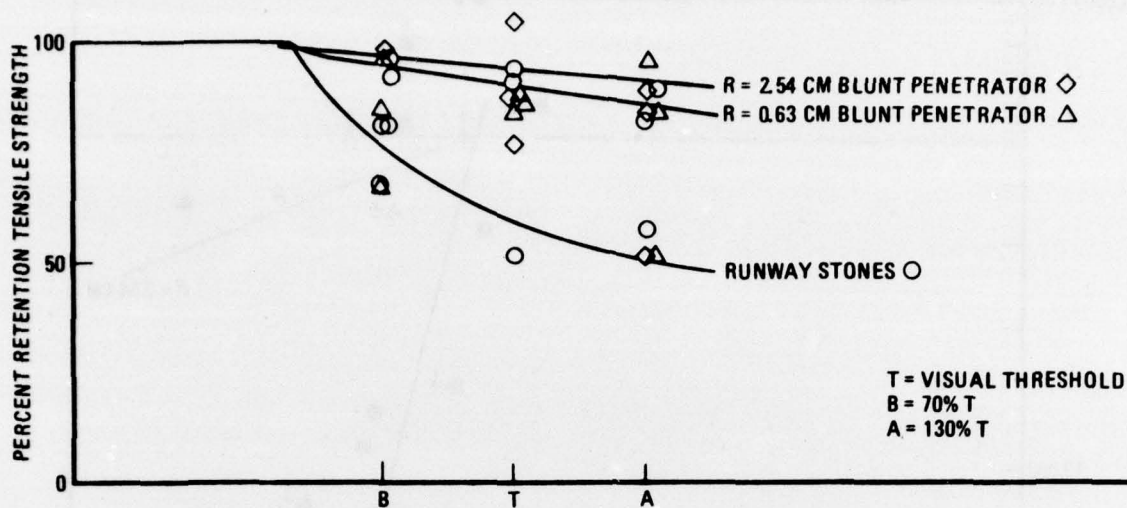Figure 5- 9. Honeycomb Panel Specimen Fatigue Results

Figure 5-10. Tensile Strength of the ISP Specimens
as a Function Damage
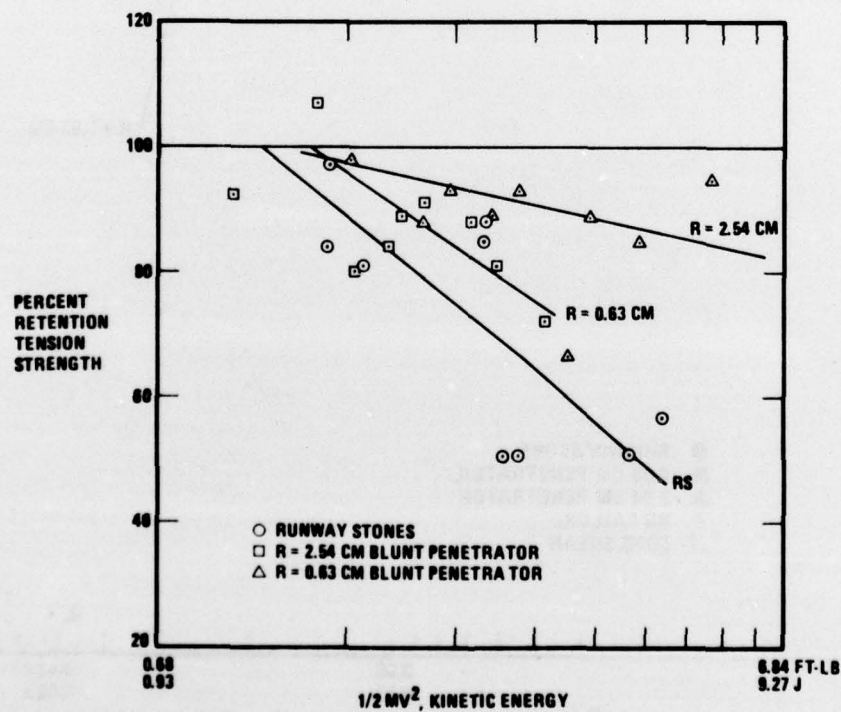

Figure 5-11. Percent Retention Tension Strength Versus Kinetic
Energy at Impact; I-Stiffened Panels
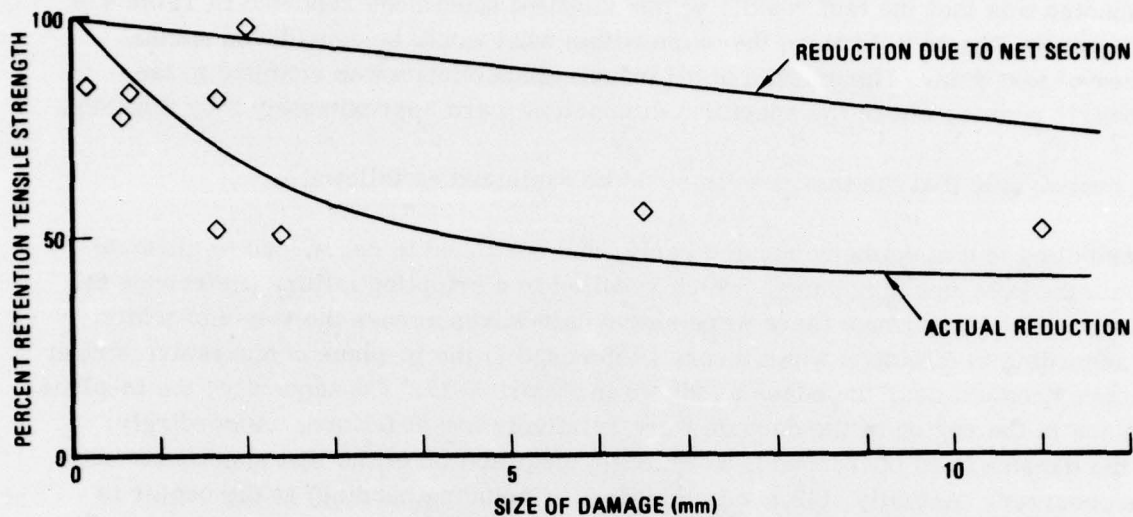
Figure 5-12. Tensile Strength as a Function of Hole Size for ISP
Specimens Damaged with Runway Stones

the holes and slots were through the thickness while in the present case it is difficult
to determine the exact size or if they were truly all the way through the specimen.
The fracture toughness of the laminate can then be computed using the equation

$$K_Q = (\frac{K_1}{K_{1\infty}})\ \sigma_N \sqrt{\pi c},$$

where K_Q = Critical stress intensity factor
K_1 = Stress intensity factor
σ_N = Net stress
c = 1/2 Crack length

(1)

which is taken from Reference 3. A second method of calculating the fracture tough-
ness is to use the standard equations for metals[4], and in that case the equation is

$$K_Q = \left\lceil 1.77\ 1-0.1\ (\frac{2R}{w}) + (\frac{2R}{w})^2 \right\rceil \sigma_G \sqrt{R}$$

where R = Radius of hole
w = Width of specimen
σ_G = Gross stress

(2)

The values calculated by these equations are substantially higher than expected for
this type of material and suggest that while the trend is correct the formula's are not
directly applicable.

The crippling specimens of the present program are similar laminate as
one of those tested in Reference 5, and the crippling strengths were expected to be
approximately equal. The two laminates were:

Present Program

$[\pm45/0_2/\mp45]_2$

Reference 5

$[\pm45_2/0_8/\mp45_2]_T$

---

4. W. F. Brown, Sr., and J. E. Srawley, Plane Strain Crack Toughness Testing
of High Strength Metallic Materials, STP410, ASTM, 1967.

As expected, the control specimens (undamaged) tested within the empirical crippling curve developed in Reference 5 as shown in Figure 5-13. What was completely unexpected was that the test results of the damaged specimens reported in Table 4-6 and shown in Figure 5-14 were the same within what would be considered normal scatter of test data. The damage of all crippling specimens was confined to the geometric center, where the specimen dimensions were approximately 2 by 8 inches.

It is conceivable that the test results could be explained as follows:

All crippling test specimens buckled early, and continued to carry load to ultimate far into the post-buckling range, which resulted in a crippling failure (Reference 6). In the post-buckling range there were single half-waves across the two-inch width, and according to effective-width theory (Reference 7) the in-plane compressive stress becomes greatest near the edges as shown in Figure 5-15. Consequently, the in-plane stresses in the region of the damage were relatively low at failure. Accordingly, had the damage been positioned near an edge, degradation of the test specimens may have occurred. Actually, the maximum stress (including bending) at the center is likely to be greater than the in-plane stress based on the findings from Reference 8, which involves the nonlinear analysis of a boron/aluminum crippling test (b/t - 20).

It is clear that damage away from the edges in large buckled skin panels would not impair the structure as long as the layup is of high integrity in compression, certainly not a unidirectional laminate; this does not necessarily apply to honeycomb sandwich compression tests. However, if the same skin panels were unbuckled up to failure, degradation would most likely occur. This would certainly apply to sandwich panels as well.

5.   "Empirical Crippling Analysis of Graphite/Epoxy Laminated Plates," paper published in Proceedings of Fourth ASTM Conference on Composite Materials: Testing and Design, May 1976.

6.   "Post Buckling Behavior of Graphite/Epoxy Laminated Plates and Channels," published in Proceedings of the Army Symposium on Solid Mechanics, 1976 – Composite Materials: The Influence of Mechanics of Failure on Design, AMMRC MS 76-2, September 1976.

7.   Th. von Karman, E. Sechler, and L. Donnell, "The Strength of Thin Plates in Compression," Trans. ASME, Vol. 54, No. 2, June 30, 1932.

8.   E. E. Spier, and G. Wang, "On Buckling of Unidirectional Boron/Aluminum Stiffeners - A Caution to Designers," J. Composite Materials, Vol. 9, October 1975.

DAMAGED SPECIMENS CRIPPLING LOADS	
(LB)	(N)
4355	19 371
4800	21 350
4875	21 684
4700	20 905
5000	22 240
4700	20 905
4610	20 505
4840	21 528
4945	21 995
4575	20 349
4750	21 128
4550	20 238
4765	21 194
4830	21 483
4650	20 683
4630	20 594
4755	21 150
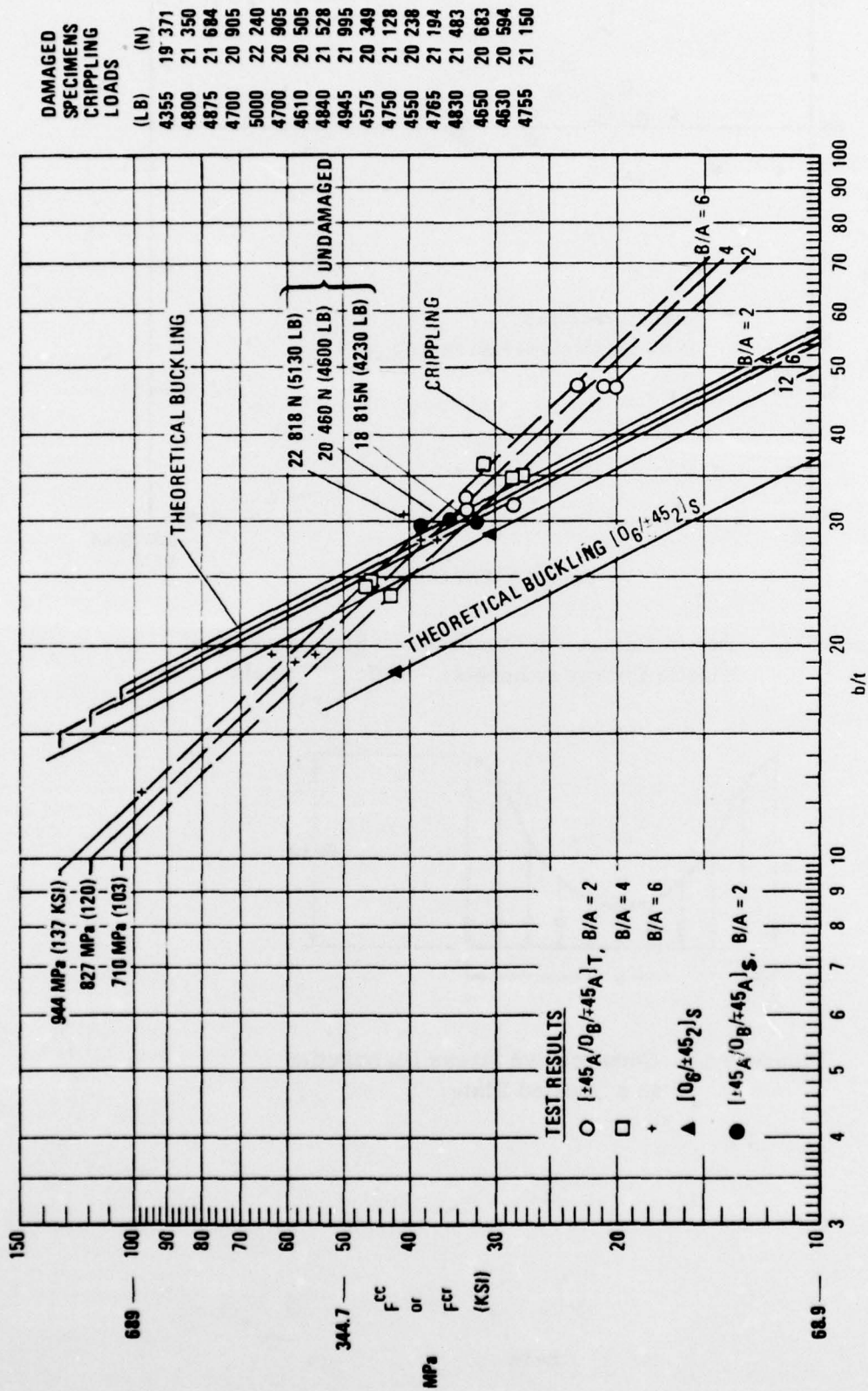
Figure 5-13. No-edge-free Crippling Curves for G/E A-S/3501 $[\pm 45_A/0_B/\mp 45_A]_T$ and $[0_b/\pm 45_2]_S$
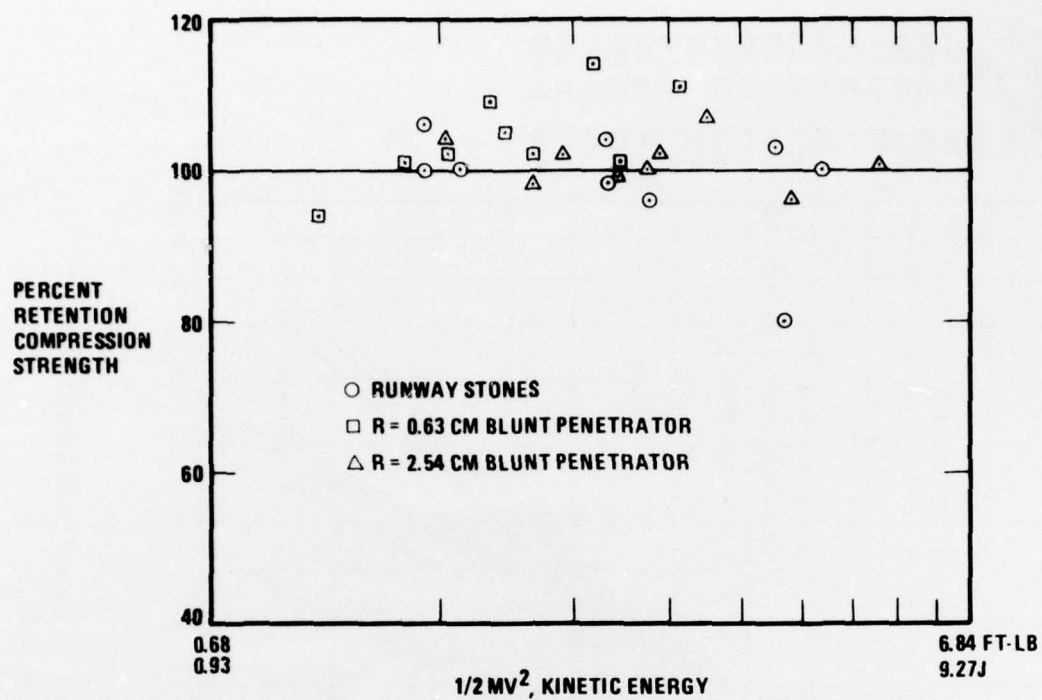
Figure 5-14. Percent Retention Compression Strength Versus
Kinetic Energy at Impact; I-Stiffened Panels
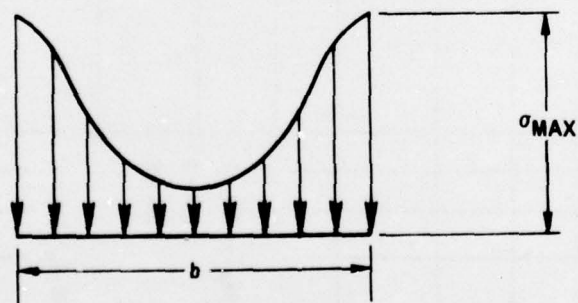
Figure 5-15. Compressive Stress Distribution
in a Buckled Plate

5-14

The fatigue test results from the laminates are intrigueing. After some difficulties with the test procedures, it was decided that tension-tension tests would be run. Almost all of the specimens survived 2.5×10^6 cycles and were then statically tested to failure. When these static results are plotted versus energy of the impactor (Figure 5-16), the same trends as observed in tension are observed. There is one slight difference in the data from the fatigued specimens. In general, it is higher than the previous static test data. This suggests that either the scatter is very large or if one believes the data, the fatigue tests are reducing the effect of the damage. While no C-scans were made of the fatigued specimens, observations on previous work on unidirectional specimens with holes indicates that the flaws propagate in the direction parallel to the specimen rather than across it. This has the effect of reducing the notch sharpness (K_t) and hence leads to a higher maximum stress. It is obvious that the specimen did not wear out nor seem to fit a wear-out model.
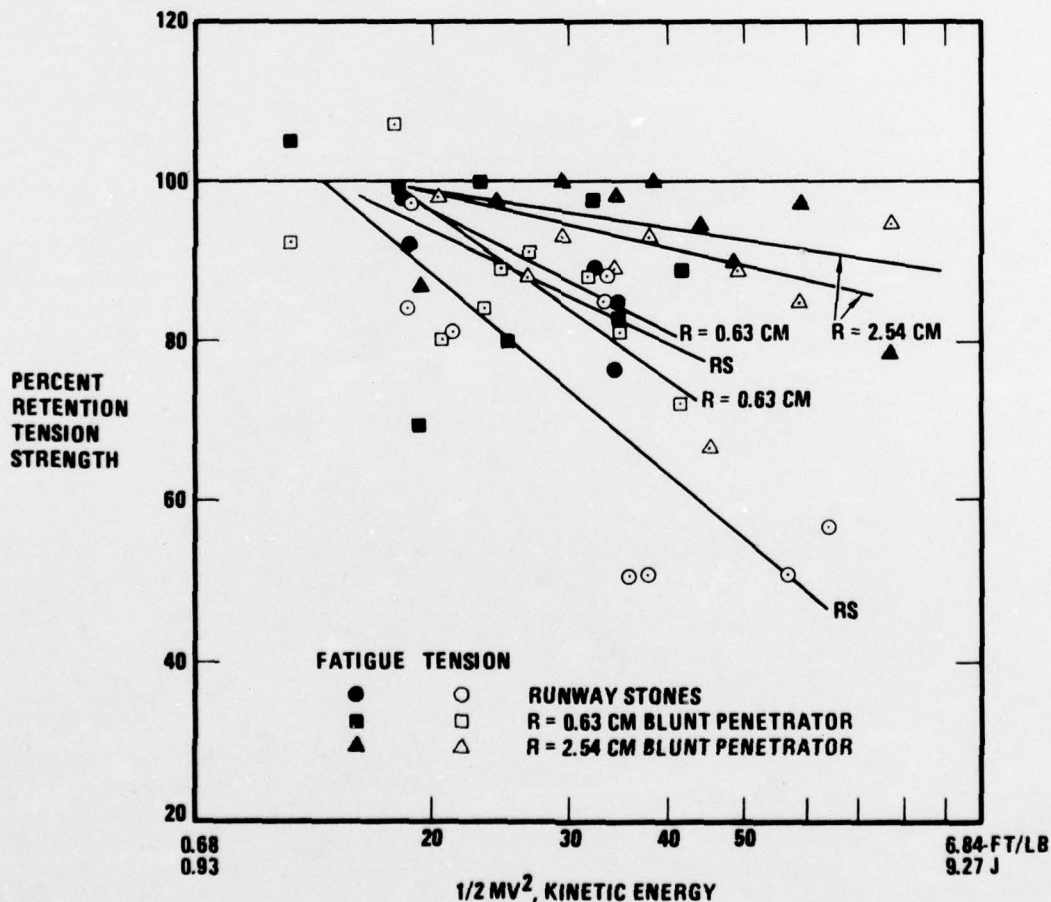
Figure 5-16. Percent Retention Tension Strength
Versus Kinetic Energy at Impact;
I-Stiffened Panels

Consistent with data from the previous tests on the static tensile specimens, the runway stones caused the most damage, followed by the sharper of the two blunt penetrators. The sharper the penetrator the more likely it is to break fibers and cause loss of strength. The delamination damage just does not seem to contribute significantly to the loss of tensile strength.

SECTION 6

CONCLUSIONS AND RECOMMENDATIONS

In any program one obtains answers but of necessity leaves some facets of the problem with less than complete answers. Such is the case in this program. The most obvious and striking fact is that service condition such as runway stones and tools can induce damage in graphite/epoxy laminate. It is also obvious that this damage does cause a loss in some measured mechanical responses of 5.04cm wide specimens. Some more quantitative conclusions include:

1. A design must be such that the structure would tolerate a 6.3mm (1/4-inch) diameter hole drilled in the structure located at random to account for sub-visual threshold damage.

2. The size of the damage, however, seems to be controlled by the energy of the threat in the visual threshold region.

3. The smaller the penetrator at identical kinetic energies the more likely it is to lead to fiber damage and subsequent loss of tensile properties.

4. The decrease in tensile strength of both flat panel and honeycomb specimens is related to the size of the damage, which, in turn is related to the energy of the threat. The trends are those expected from fracture mechanics but the values seem rather large.

5. Tension-tension fatigue of the flat panel laminates suggests that this may blunt the stress concentration by changing the crack shape. This agrees with previous work on other composites.

6. The compression strength of the honeycomb panels with 88 kg/m^3 (5.5 pcf) HRP core is decreased in relation to the energy of the threat. This was correlated to the damage of the core, which caused a loss of stability of the G/E facesheets.

7. The compression strength of center damaged flat panels tested in crippling with a b/t of 30 showed no changes in strength. Analytical methods indicate this is due to the buckling of the panel and that if the damage is near (not at) an edge, the decrease would have been substantial.

8. The fatigue tests of the honeycomb panels show what appeared to be some growth of the damage. The results also suggest that the damage must have grown.

9. The modulus of elasticity (stiffness) of the material did not seem to be affected by the damage. The strain to failure was a function of the damage.

Several areas were not explored. More work needs to be directed at finding answers to the following:

1. This study used dried specimens only. Work needs to be directed at finding the effect of moisture.

2.   Some of this work suggests that the flaws can grow and change the damage. More quantitative work needs to be directed at measuring the flaw growth rate.

3.   The measured reduction in strengths of the 5.4cm (2-inch) wide specimens was substantial. Some work needs to be undertaken to define the effect of specimen size. The change in the boundary conditions (impacts near stiffeners versus away from stiffener) had a great effect on the damage induced in the laminate. More work needs to be directed at this problem.

5.   The core greatly influence the effect of the damage on the honeycomb panels. The effect of less brittle cores, such as aluminum, needs to be studied.

6.   A direct comparison between an I-stiffened panel and a honeycomb panel needs to be made. Panels need to be made to take the same boundary loads and then be hit with the same threat to determine which type of construction is the most damage tolerant.

7.   Finally, the percent reduction in load carrying capability of the G/E structures appears to be large. The relative loss in load carrying capability of comparable aluminum structure needs to be determined to see how much more (or less) vulnerable G/E is to low velocity impact than is aluminum.

DISTRIBUTION LIST

Government Activities

NAVAIRSYSCOM, AIR-954 (2 for retention), 2 for AIR-530,
  1 for AIR-320B, AIR-52032D, AIR-5302, AIR-53021, AIR-530215). .   9

NAVSEASYSCOM, Washington, D. C. 20362
  (Attn: Code 035, Mr. C. Pohler).   1

NAVSEC, Hyattsville, MD 20782
  (Attn: Code 6101E03, Mr. W. Graner).   1

ONR, Washington, D. C. 20362
  (Attn: Dr. N. Perrone)   1

NAVSHIPRANDCEN, Bethesda, MD 20034
  (Attn: Code 173.2, Mr. W. P. Cauch).   1

NAVSHIPRANDCEN, Annapolis, MD 21402
  (Attn: Code 2870, Mr. H. Edelstein).   1

NOL, White Oak, MD 20910
  (Attn: Mr. F. R. Barnet).   1

NRL, Washington, D. C. 20375
  (Attn: Dr. I. Wolock).   1

NAVPGSCHL, Monterey, CA 95940
  (Attn: Prof. R. Ball, Prof M. H. Bank)   2

AFOSR, Washington, D. C. 20333
  (Attn: Mr. J. Pomerantz)   1

AFML, WPAFB, OH 45433
  (Attn: LAM (Technical Library)).   1
  (Attn: LT-1/Mr. W. R. Johnston).   1
  (Attn: LTF/Mr. T. Cordell)   1
  (Attn: FBSC/Mr. L. Kelly).   1
  (Attn: MAC/Mr. G. P. Peterson)   1
  (Attn: MXA/Mr. F. J. Fechek)   1
  (Attn: MBC/Mr. T. G. Reinhard, Jr)   1

AFFDL, WPAFB, OH 45433
  (Attn: FB/Mr. P. A. Parmley)   2
  (Attn: FBC/Mr. C. Wallace)   1
  (Attn: FBC/Mr. E. E. Zink)   1

USAMATRESAG, Watertown, MA
  (Attn: Dr. E. Lenoe)   1

USARESOFC, Durham, NC 27701   1

USAAVMATLAB, Fort Eustis, VA 23603
  (Attn: Mr. R. Beresford)   1

PLASTEC, Picatinny Arsenal, Dover, NJ 07801
  (Attn: Librarian, Bldg. 176, SARPA-FR-M-D and Mr. H. Pebly). .   2

NASA (ADM), Washington, D.C. 20546
  (Attn: Secretary).   1

Naval Air Development Center, Warminster, PA 18974
  (Attn: Receiving Officer, AVTD (Code 3033) . . . . remainder
                                           req'd under contract

Government Activities (Cont.)

Scientific & Technical Information Facility, College Park, MD
    (Attn: NASA Representative). 1
NASA, Langley Research Center, Hampton, VA 23365
    (Attn: Mr. J. P. Peterson, Mr. R. Pride, and Dr. M. Card). . . . 3
NASA, Lewis Research Center, Cleveland, OH 44153
    (Attn: Tech. Library). 1
NASA, George C. Marshall Space Flight Center, Huntsville,
   AL 35812
    (Attn: S & E-ASTN-ES/Mr. E. E. Engler) 1
    (Attn: S & E-ASTN-M/Mr. R. Schwinghamer) 1
    (Attn: S & E-ASTM-MNM/Dr. J. M. Stuckey) 1
DDC. 12
FAA, Airframes Branch, FS-120, Washington, D. C. 20553
    (Attn: Mr. J. Dougherty) 1

Non-Government Agencies

Avco Aero Structures Division, Nashville, TN 37202
    (Attn: Mr. W. Ottenville). 1
Avco Space Systems Division, Lowell, MA 01851
    (Attn: Dr. M. J. Salkind). 1
Bell Aerospace Company, Buffalo, NY 14240
    (Attn: Zone I-85, Mr. F. M. Anthony) 1
Bell Helicopter Company, Fort Worth, TX 76100
    (Attn: Mr. Charles Harvey). 1
Bendix Products Aerospace Division, South Bend, IN 46619
    (Attn: Mr. R. V. Cervelli) 1
Boeing Aerospace Company, P.O. Box 3999, Seattle, WA 98124
    (Attn: Code 206, Mr. R. E. Horton) 1
Boeing Company, Renton, Washington 98055
    (Attn: Dr. R. June). 1
Boeing Company, Vertol Division, Phila., PA 19142
    (Attn: Mr. R. L. Pinckney, Mr. D. Hoffstedt) 2
Boeing Company, Wichita, KS 67210
    (Attn: Mr. V. Reneau/MS 16-39) 1
Cabot Corporation, Billerica Research Center, Billerica, MA
   01821 1
Drexel University, Phila., PA 19104
    (Attn: Dr. P. C. Chou) 1
E. I. DuPont Company, Wilmington, DE 19898
    (Attn: Dr. Carl Zweben) Bldg. 262/Room 316 1
Fairchild Industries, Hagerstown, MD 21740
    (Attn: Mr. D. Ruck). 1
Ferro Corporation, Huntington Beach, CA 92646
    (Attn: Mr. J. L. Bauer). 1
Georgia Institute of Technology, Atlanta, GA
    (Attn: Prof. W. H. Horton) 1

General Dynamics/Convair, San Diego, CA 92138
 (Attn: Mr. D. R. Dunbar, W. G. Scheck) 2
General Dynamics, Fort Worth, TX 76101
 (Attn: Mr. P. D. Shockey, Dept. 23, Mail Zone P-46). 1
General Electric Company, Phila., PA 19101
 (Attn: Mr. L. McCreight) 1
Great Lakes Carbon Corp., N.Y., NY 10017
 (Attn: Mr. W. R. Benn, Mgr., Markey Development) 1
Grumman Aerospace Corporation, Bethpage, L.I., NY 11714
 (Attn: Mr. R. Hadcock, Mr. S. Dastin). 2
Hercules Powder Company, Inc., Cumberland, MD 21501
 (Attn: Mr. D. Hug) 1
H. I. Thompson Fiber Glass Company, Gardena, CA 90249
 (Attn: Mr. N. Myers). 1
ITT Research Institute, Chicago, IL 60616
 (Attn: Dr. R. Cornish). 1
J. P. Stevens & Co., Inc., N.Y., NY 10036
 (Attn: Mr. H. I. Shulock). 1
Kaman Aircraft Corporation, Bloomfield, CT 06002
 (Attn: Tech. Library). 1
Lehigh University, Bethlehem, PA 18015
 (Attn: Dr. G. C. Sih). 1
Lockheed-California Company, Burbank, CA 91520
 (Attn: Mr. E. K. Walker, R. L. Vaughn) 2
Lockheed-Georgia Company, Marietta, GA
 (Attn: Advanced Composites Information Center, Dept. 72-14,
    Zone 42). 1
LTV Aerospace Corporation, Dallas, TX 75222
 (Attn: Mr. O. E. Dhonau/2-53442, C. R. Foreman). 2
Martin Company, Baltimore, MD 21203
 (Attn: Mr. J. E. Pawken) 1
Materials Sciences Corp., Blue Bell, PA 19422 1
McDonnell Douglas Corporation, St. Louis, MO 63166
 (Attn: Mr. R. C. Goran, O. B. McBee, C. Stenberg). 3
McDonnell Douglas Corporation, Long Beach, CA 90801
 (Attn: H. C. Schjelderup, G. Lehman) 2
Minnesota Mining and Manufacturing Company, St. Paul, MN 55104
 (Attn: Mr. W. Davis) 1
Northrop Aircraft Corp., Norair Div., Hawthorne, CA 90250
 (Attn: Mr. R. D. Hayes, J. V. Noyes, R. C. Isemann). 3
Rockwell International, Columbus, OH 43216
 (Attn: Mr. O. G. Acker, K. Clayton). 2
Rockwell International, Los Angeles, CA 90053
 (Attn: Dr. L. Lackman) 1
Rockwell International, Tulsa, OK 74151
 (Attn: Mr. E. Sanders, Mr. J. H. Powell) 2
Owens Corning Fiberglass, Granville, OH 43023
 (Attn: Mr. D. Mettes). 1

Rohr Corporation, Riverside, CA 92503
   (Attn: Dr. F. Riel and Mr. R. Elkin) 2
Ryan Aeronautical Company, San Diego, CA 92112
   (Attn: Mr. R. Long). 1
Sikorsky Aircraft, Stratford, CT 06497
   (Attn: Mr. J. Ray) 1
Southwest Research Institute, San Antonio, TX 78206
   (Attn: Mr. G. C. Grimes) 1
University of Oklahoma, Norman, OK 93069
   (Attn: Dr. G. M. Nordby) 1
Union Carbide Corporation, Cleveland, OH 44101
   (Attn: Dr. H. F. Volk) 1
Battelle Columbus Laboratories, Metals and Ceramics Information
   Center, 505 King Avenue, Columbus, OH 43201. 1